



저작자표시-비영리-변경금지 2.0 대한민국

이용자는 아래의 조건을 따르는 경우에 한하여 자유롭게

- 이 저작물을 복제, 배포, 전송, 전시, 공연 및 방송할 수 있습니다.

다음과 같은 조건을 따라야 합니다:



저작자표시. 귀하는 원저작자를 표시하여야 합니다.



비영리. 귀하는 이 저작물을 영리 목적으로 이용할 수 없습니다.



변경금지. 귀하는 이 저작물을 개작, 변형 또는 가공할 수 없습니다.

- 귀하는, 이 저작물의 재이용이나 배포의 경우, 이 저작물에 적용된 이용허락조건을 명확하게 나타내어야 합니다.
- 저작권자로부터 별도의 허가를 받으면 이러한 조건들은 적용되지 않습니다.

저작권법에 따른 이용자의 권리는 위의 내용에 의하여 영향을 받지 않습니다.

이것은 [이용허락규약\(Legal Code\)](#)을 이해하기 쉽게 요약한 것입니다.

[Disclaimer](#)

Dissertation for the Degree of
Master of Landscape Architecture

Distribution Change of Conifer and
Broad-leaved Tree and Predict Future
Distribution at Namsan (Mt.), Sangju

상주시 남산 활엽수와 침엽수의 과거 분포 변화
분석 및 미래 분포 예측

February 2016

Graduate School of Seoul National University
Department of Landscape Architecture and
Rural System Engineering

Han Kyul Heo

■ Abstract

Distribution Change of Conifer and Broad-leaved Tree and Predict Future Distribution at Namsan (Mt.), Sangju

Advisor Prof. : Lee, Dongkun
Seoul National University
Department of Landscape Architecture
Heo, Hankyul

Researches about analyzing and predicting distribution of forest are continuously proceeded in aspect of a forest management. To analyze the past distribution of forest, researchers record data about forest distribution and characteristics like forest inventory. However, these data couldn't provide long term data. Therefore, remote sensing was used to construct data. Landsat image which is remotely sensed data was used because Landsat image is appropriate to analyze the forest.

Conifer and broad-leaved tree in Namsan, Sangju-si was analyzed for thirty years. As a result, distribution of broad-leaved tree was continuously increasing, on the other hand, conifer was decreased. Forest distribution was highly affected by human activity which is heating in the past. Therefore, broad-leaved tree which is more appropriate for fire wood was distributed in small area.

Predicting future distribution was proceeded based on modelling

method. Researches that based on niche model predict suitable habitat, and researches based on process-based models and demographic models predict real distribution. However, these methods have limitations in forest management because niche model cannot predict real distribution and process-based model and demographic model predict in large scale because of the scale of input data. This research aims to overcome this limitation by predicting future distribution of conifer and broad-leaved tree. Because conifer and broad-leaved tree are typical species which is in competition and conifer is weak competitor.

In this research, present distribution of conifer and broad-leaved tree and replacement probability of conifer by broad-leaved tree was used to predict future distribution. Probability of conifer by broad-leaved tree was modelled based on logistic regression model using forest distributions from past to present. Remote sensing was used to construct data because forest distribution is changing slowly and satellite images provide long periodic data. Furthermore, Landsat images were selected because of fine spatial scale and long temporal extent.

Past distribution map was constructed by using classification method. Comparing past distribution of conifer and broad-leaved tree maps for the periods 1984-1995, 1995-2005, and 2005-2014, classes that represented either a 'conifer to broad-leaved tree' or 'conifer to conifer' change were generated. For logistic regression, distribution changed maps were used for dependent variable and distance from

broad-leaved forest edge, elevation, slope, topographic wetness index (TWI), annual solar radiation were used for independent variable.

Compare the result of distribution changed map with previous researches, distance variable which used in this research seems suitable factor to predict distribution change. Most replacement of conifer by broad-leaved tree was occurred near broad-leaved forest edges and decreases sharply similar to seed dispersal and seed density pattern of other researches.

However, distance was calculated based on 30m spatial resolution, therefore, the distance from broad-leaved forest edge has uncertainties. To overcome this uncertainty, Monte Carlo simulation was used. According to simulation result range of distance value was considered.

As a result of logistic regression, annual solar radiation and distance from broad-leaved forest edge were turn out to be powerful factor to predict replacement probability of conifer by broad-leaved tree. In other words, replacement probability of conifer by broad-leaved tree was increased where close to broad-leaved forest edge and annual solar radiation is low. It reflects the seed dispersal and density of seed that density of seed is higher near the broad-leaved forest edge. In addition, it reflects the characteristic of conifer and broad-leaved tree that shade tolerance of conifer is weaker than broad-leaved tree.

Future distribution of conifer and broad-leaved tree was predicted by using the result of logistic regression model. Distribution of conifer will decrease slowly than before. broad-leaved tree population

curve seems similar to sigmoid curve which known as population growth model. It is considered that forest area comes to limited resource, therefore, competition was occurred between conifer and broad-leaved tree.

As a result, distance was turn out to be an important variable to predict future distribution. Using the distance from broad-leaved forest edge, it is possible to predict future distribution of conifer and broad-leaved tree. Furthermore, to overcome the uncertainty due to spatial resolution, it is possible to use Monte Carlo simulation.

keywords : Remote sensing, Logistic regression, Topographic correction, Monte carlo simulation, Uncertainty

Student Number : 2014-20047

Table of contents

Table of contents	i
List of tables	iii
List of figures	iv
1. Introduction	1
2. Literature Reviews	4
2.1 Remote sensing	4
2.2 Forest distribution prediction	7
2.3 Seed dispersal	10
3. Research Methodology	13
3.1 Scope of the study	13
3.2 Materials and method	15
3.2.1 Study flow	15
3.2.2 Study material	16
3.2.3 Method	18
4. Result and Discussion	27
4.1 Remote sensing	27

4.1.1 Pre-processing	27
4.1.2 Image classification	27
4.2 Logistic regression	33
4.2.1 Constructing variable	33
4.2.2 Logistic regression model	37
4.2.3 Considering uncertainty	41
4.2.4 Distribution prediction	43
4.2.5 Distribution prediction considering uncertainty in distance	46
5. Conclusions	49
6. References	52
7. Appendix	59
국문초록	62

List of tables

Table 1. Comparison of the satellite images	4
Table 2. Number of saplings depends on distance	12
Table 3. Dependent variable for logistic regression	17
Table 4. The parameters value used for the FLAASH algorithm	19
Table 5. Interpretation key	21
Table 6. The parameters used for the area solar radiation	23
Table 7. Variables for logistic regression	24
Table 8. Covered area of conifer and broad-leaved tree	28
Table 9. ROI accuracy and kappa coefficient	31
Table 10. Error matrix for 2014	31
Table 11. Error matrix for 2008	32
Table 12. Statistical result of frequency analysis	36
Table 13. Result of correlation coefficient analysis	38
Table 14. Result of logistic regression analysis	39
Table 15. statistics of logistic regression model	39
Table 16. Error matrix of logistic regression model	40
Table 17. Result of logistic regression analysis (model A)	43
Table 18. Result of logistic regression analysis (model B)	43
Table 19. Result of logistic regression analysis (model C)	43
Table 20. Predicted covered for each model	47

List of figures

Figure 1. Suitable range considering three climate index	8
Figure 2. Site-scale process	9
Figure 3. Individual scale process	9
Figure 4. Relationship between seed density and distance from parent ...	10
Figure 5. Density difference between homogeneous landscape and heterogeneous landscape	11
Figure 6. Study area	13
Figure 7. Research flow	15
Figure 8. Euclidean distance between two cell	25
Figure 9. Distance between two cell	25
Figure 10. Pre-processing results (false color)	27
Figure 11. Result of classification	28
Figure 12. Classification result and residential area	29
Figure 13. Independent variables	34
Figure 14. Distance from broad-leaved forest edge	35
Figure 15. Graph of replacement ratio and distance from broad-leaved forest edge	37
Figure 16. ROC curve	41
Figure 17. Histogram of simulation	42
Figure 18. Predicted distribution at 2024	44
Figure 19. Predicted distribution at 2034	45
Figure 20. Covered area change of conifer and broad-leaved tree	46
Figure 21. Covered area of conifer and broad-leaved tree	48

1. Introduction

Forests play important roles in regulating the environment, and they cover approximately 30% of Earth's land surface (Muraoka, 2015). In Korea, 64% of the terrestrial area is covered by forests, making forest management an important discipline, especially the monitoring and predicting of forest distributions (Ge et al., 2013). Distribution change through time can be analysed by using forest inventory data. However, in case of distribution change in lengthy period of time, forest inventory data is not constructed enough period.

Remote sensing has great advantages of vegetation analysis because of reflectance characteristics of near-infrared (Song and Shin, 2000). Long period forest distribution data can be constructed using remote sensed data. Therefore, forest distribution change was studied with remote sensed satellite images (Song et al., 2007; hmann et al., 2012).

In addition, predicting forest distribution is therefore considered an important research area by international institutions (Joshi et al., 2014), and research on forest distribution predictions has progressed in recent years. To predict distributions, there are three main types of modeling methods: niche based models, process-based models, and demographic models (Beale and Lennon, 2012). Niche based models use environmental variables based on statistical techniques, although they cannot reflect species interactions (Franklin, 2009), which is an important factor for predicting species distributions (Ryu and Lee, 2002).

Studies to overcome this shortcoming have been conducted by comparing the habitat suitability among species or functional types (Choi et al., 2011; Kwak et al., 2012). By using this method, predicting distributions for more than two species in competition is therefore possible, resulting in predictions of potentially suitable habitats.

Process-based models and demographic models not only explain dispersal ability, but also dynamic processes like birth rate, death rate, plant size, plant density, and environmental resources (Moorcroft et al., 2001; Beale and Lennon, 2012). Generally, these models are using environmental variables such as topographic condition, solar radiation, soil type, or plants characteristics. Especially, seed dispersal was turn out to be an important factor to predict plant distribution change (Liang et al., 2015).

Namsan (Mt.) is located at Sangju-si, Gyeongsangbuk-do. Namsan was almost bare mountain because trees were used for fire wood. Therefore, afforestation was conducted in 1979–1980 around deforested area, using conifer and Japanese alder (*Alnus japonica*). However, Japanese alder was removed after the afforestation because of low economic feasibility. For now, surveyed data shows that pine and *Quercus* spp. are dominant tree in Namsan which is typical species that are in competition (Lee et al., 2006; Byun et al., 2010).

Past distribution of conifer and broad-leaved tree at Namsan (Mt.) were analyzed and future distributions of conifer and broad-leaved tree at Namsan (Mt.) were predicted in this research. The

replacement probability of conifer by broad-leaved tree was used, so that predictions of future distributions of both tree could be based on past replacement patterns. Therefore, this research used remote sensing data to compute replacement patterns from the past, since remote sensing data can provide long periodic data for forest studies (Huang et al., 2009; Sexton et al., 2013; Song et al., 2014). Overall, in this study, future distribution patterns of conifer and broad-leaved tree were predicted based on past changing pattern.

2. Literature reviews

2.1 Remote sensing

Remote sensing is a tool for collecting data without making physical contact (Liu and Mason, 2009). Optical remote sensing system measured solar energy reflected from materials surface (Reddy, 2008). IKONOS, Quickbird, WorldView, KOMPSAT, Landsat, Hyperion, ASTER and SPOT is a typical earth observation satellite images (Table 1).

Table 1. Comparison of the satellite images

Satellite	Launched year	Spectral range	Resolution
IKONOS	1999	526–929nm(panchromatic) 445–516nm(blue) 506–595nm(green) 632–698nm(red) 757–853nm(NIR)	Pan: 1m Multi spectral: 4m
Quickbird	2001	405–1,053nm(panchromatic) 430–545nm(blue) 466–620nm(green) 590–710nm(red) 715–918nm(NIR)	Pan: 0.61m Multi spectra: 2.44m
WorldView–2	2009	450–800nm(panchromatic) 400–450nm(coastal) 450–510nm(blue) 510–580nm(green) 585–625nm(yellow) 630–690nm(red) 705–745nm(red edge) 770–895nm(NIR1) 860–1,040nm(NIR2)	Pan: 0.46m Multi spectra: 1.85
KOMPSAT–2	2006	500–900nm(panchromatic) 450–520nm(blue) 520–600nm(green) 630–690nm(red) 760–900nm(NIR)	Pan: 1m Multi spectra: 4m
Landsat	1972	0.5–0.6 μ m(green) 0.6–0.7 μ m(red)	Multi spectra: 80m

		0.7–0.8 μm (IR) 0.8–1.1 μm (IR)	
Landsat TM	1982	0.45–0.52 μm (blue) 0.52–0.60 μm (green) 0.63–0.69 μm (red) 0.76–0.90 μm (IR) 1.55–1.75 μm (IR) 10.4–12.5 μm (TIR) 2.08–2.35 μm (IR)	Multi spectra: 30m TIR: 120m
Landsat ETM+	1999	0.45–0.515 μm (blue) 0.525–0.605 μm (green) 0.63–0.69 μm (red) 0.75–0.90 μm (IR) 1.55–1.75 μm (IR) 10.4–12.5 μm (TIR) 2.08–2.35 μm (IR) 0.52–0.9 μm (panchromatic)	Pan: 15m Multi spectra: 30m TIR: 120m
Hyperion	2000	357–2,576nm	Multi spectra: 30m
SPOT	1986	450–745nm(panchromatic) 450–525nm(blue) 530–590nm(green) 625–695(red) 760–890nm(NIR)	Pan: 10m Multi spectra: 20m

IR: Infrared, NIR: Near-infrared, TIR: Thermal Infrared
Modified from Park et al.(2011)

Especially remote sensing has great advantages of vegetation analysis because of reflectance characteristics of near-infrared (Song and Shin, 2000). NDVI (Normalised Difference Vegetation Index), which is computed using red and near-infrared band, indicates the presence and condition of vegetation (Reddy, 2008). Therefore, vegetation area and non vegetation area can classified by using NDVI (Defries and Townshend, 1994; Jia et al., 2014). Furthermore, ecological responses to environmental change could be observed (Pettorelli et al., 2005). In other words, it is possible to classify land cover between vegetation and non vegetation.

Furthermore, we can observe forest cover change using remote sensing. Kim et al. (2014) analyse global forest cover change from 1990 to 2000 based on Landsat image, and Leinenkugel et al. (2015) analyse Mekong basin forest cover change from 2001 to 2011 based on MODIS and Landsat image. Similarly, Song et al. (2015) analyse eastern United States and central Brazil forest cover change from 1960 to 2000 based on Landsat image. Studies used a common images which is Landsat because it is suitable for forest mapping (van der Marrel and Franklin, 2013). Consequently, Landsat image is great source of information for observing historical changes of forest cover. However, these studies cannot distinguish between evergreen tree and deciduous tree.

To distinguish between evergreen tree and deciduous tree, we can use existing data (Song and Shin, 2000). However, it has some disadvantages if data is hard to acquire.

Plant phenology was used to distinguish between evergreen tree and deciduous tree. NDVI reflects phenological aspect of plant (Jönsson and Eklundh, 2002; Pettorelli et al., 2005). In addition, deciduous tree fall leaves at winter, while evergreen tree doesn't. Therefore, greenness of tree is different after deciduous tree fell leaves (Suzuki et al., 2001). However, using remote sensing at winter is not appropriate for analysis. Because, in Korea, mountain was crowned with snow at winter. Consequently, satellite images at autumn is great source of information for observing forest cover (Joshi et al., 2014).

2.2 Forest distribution prediction

Species distribution modeling, which is method to predict species distribution, has been distinguished between ecological niche model and habitat suitability model (Franklin, 2009). Ecological niche model analyze the relationship between species occurrence data and environmental variables, and is commonly used to predict species distribution (Franklin, 2009; Song and Kim, 2012). Ecological niche model has been described both statistical model and machine learning model depending on predicting method.

However, species distribution modeling cannot reflect species interactions such as competition (Franklin, 2009). because each species have their own niche, species competition will occur, if species niche has overlapped between species(Ryu and Lee, 2002). As a result of competition, superior species can maintain their fundamental niche, however, inferior species niche will be decreased.

Habitat suitability index is used to predict more than two species distribution. Habitat suitability indices can be used to predict plant species distribution by analyzing the relationship between species occurrence data and environmental variable statistically. Furthermore, it is possible to predict more than two species distribution comparing each species habitat suitability index (Figure 1) (Choi et al., 2011; Kwak et al., 2012).

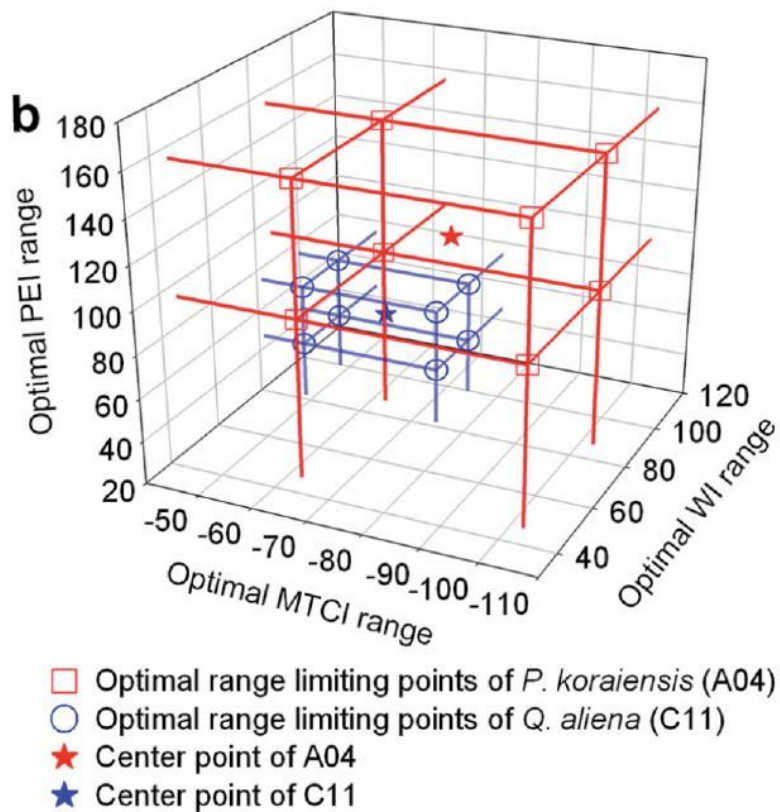


Figure 1. Suitable range considering three climate index (Choi et al., 2011)

As well as habitat suitability index, process-based models can predict more than two species. Seed dispersal, plant density, mortality rate, colonization rate and plant growth is considered in process-based model (Tilman and Kareiva, 1997) and demography model (Moorcroft et al., 2001; Liang et al., 2015). These models consider the site-scale (Figure 2) and individual scale process (Figure 3). These models are based on highly fine scale process. However, it is difficult to obtain or construct input data. Furthermore, it is too

difficult to collect each species characteristic. Therefore, most results have large scale and low resolution.

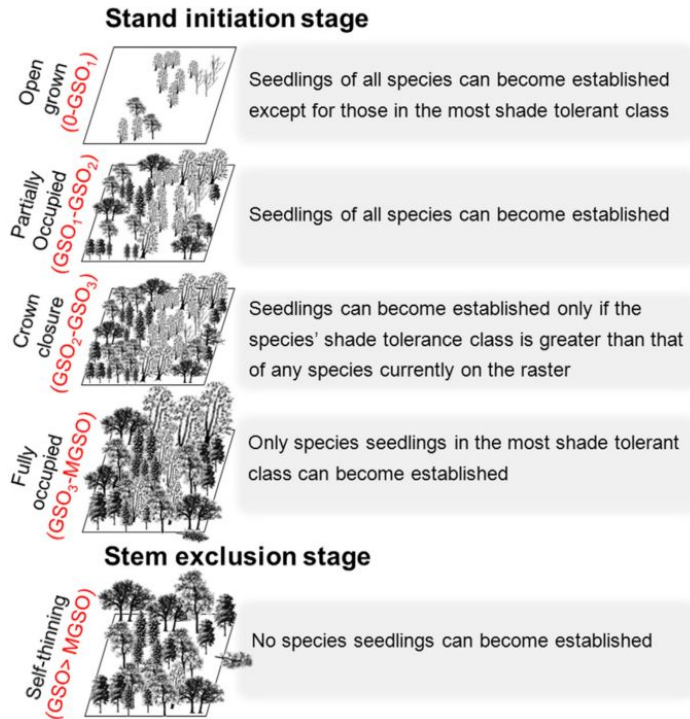


Figure 2. Site-scale process (Liang et al., 2015)

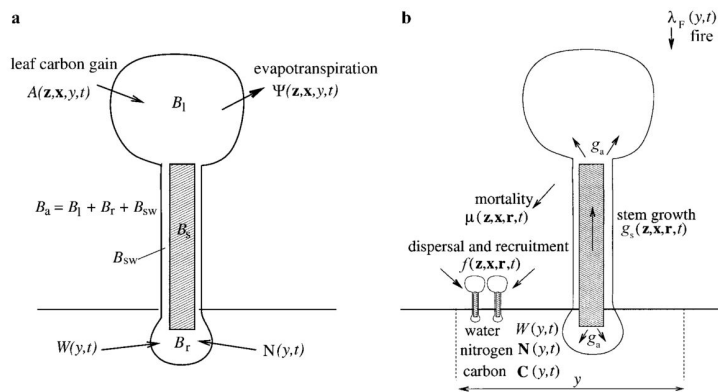


Figure 3. Individual scale process (Moorcroft et al., 2001)

2.3 Seed dispersal

With local seed dispersal, spatial pattern forms. Seed dispersal is important processes determining the spatial pattern of forest and forest dynamics (Willson, 1992; Nathan and Muller-Landau, 2000). Moving distance of seed can be estimated by analyzing the distance from parent individual to seed. Seed shadow is a spatial distribution of seeds around parents. Therefore, to analyze the seed dispersal ability, we can consider seed shadow (Willson, 1992). Generally, seed density declines leptokurtically with distance (Figure 2) (Nathan and Muller-Landau, 2000).

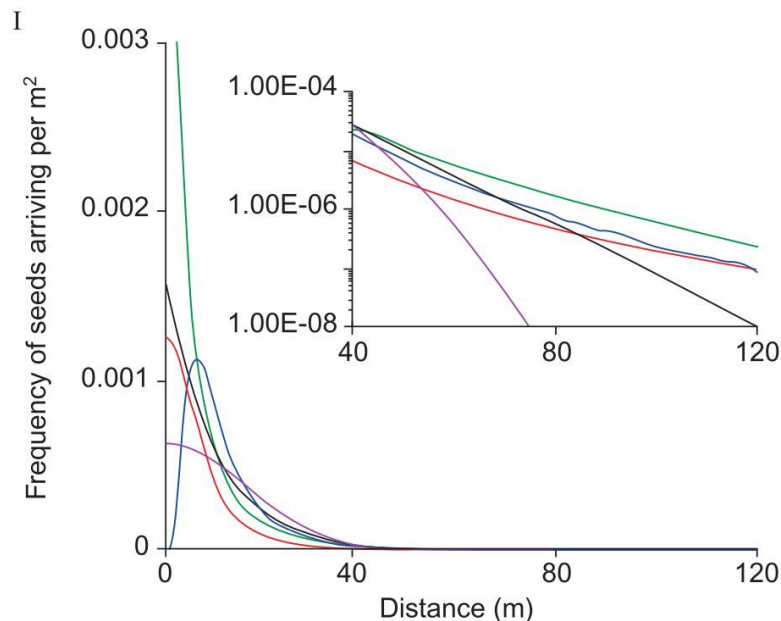


Figure 4. Relationship between seed density and distance from parent (Nathan and Muller-Landau, 2000)

Longer than 150m dispersal is called long distance dispersal (Levey

et al., 2008). In contrast to short distance dispersal, long distance dispersal occur hardly (Clark et al., 1999). Despite of low occurrence rate, long distance dispersal play important role in ecosystem(Cain et al., 2000). Like short distance dispersal, seed density of long distance dispersal declines leptokurtically with distance. However, seeds might go through more landscape elements than short distance dispersal (Levey et al., 2008). Therefore, in case of long distance dispersal, seed shadow seems varied when seeds go through various landscape elements (Figure 3).

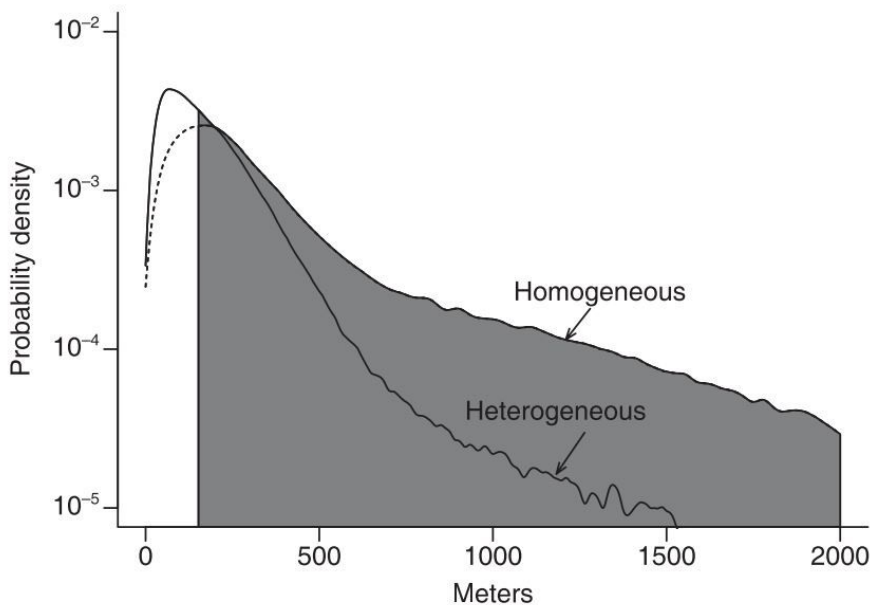


Figure 5. Density difference between homogeneous landscape and heterogeneous landscape (Levey et al., 2008)

In addition to seed shadow, we can examine spatial distribution of parent and their saplings. Dow and Ashley (1996) studied seed

dispersal of bur oak (*Quercus macrocarpa*) which is one kind of broad-leaved tree by analyzing spatial distribution of parent and their saplings. As a result, seed density declines with distance (Table 2). Therefore, it is suitable for predicting oak distribution change considering seed dispersal.

Table 2. Number of saplings depends on distance (Dow and Ashley, 1996)

Range(m)	Count	%
0-15	65	69.15
15-30	12	12.77
30-45	3	3.19
45-60	2	2.13
60-75	1	1.06
75-90	4	4.26
90-105	2	2.13
105-120	2	2.13
120-135	1	1.06
135-150	1	1.06
150-165	1	1.06

Liang et al. (2015) predict future distribution considering seedling establishment, competition, mortality and tree growth. In site-scale process, shade tolerance, growth rate, and seed dispersal turn out to important.

3. Research methodology

3.1 Scope of the study

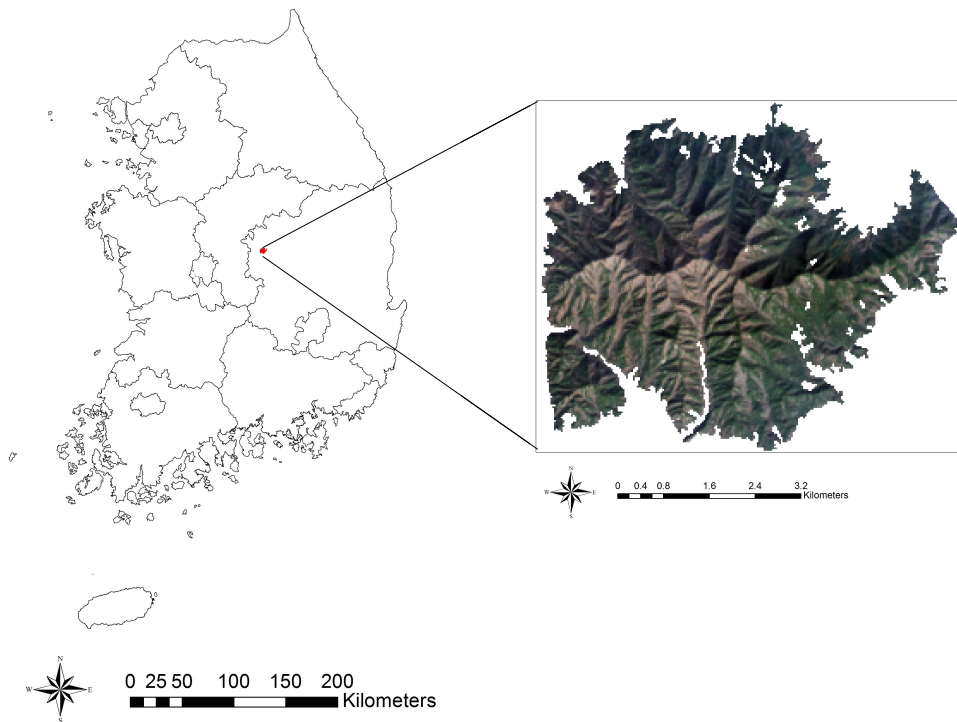


Figure 6. Study area

The study area was located in Sangju-si Gyeongsangbuk-do, which falls within Landsat path 115 and row 35 (Figure 6). The study area contains conifer (*Pinus densiflora*) and broad-leaved tree, with the latter being composed of cork broad-leaved tree (*Quercus variabilis*), sawtooth broad-leaved tree (*Quercus acutissima*), and mongolian broad-leaved tree (*Quercus mongolica*). Since the study area did not contain other species besides conifer and broad-leaved tree, it is very

suitable for the aim of the study, as effects of other plants did not have to be taken into account (Appendix. Figure S-1).

The study covered the period between 1984 and 2014. Because forest distributions change on a long-term time scale, and the detection of change requires a fine spatial scale, Landsat images were selected for this study. Given Landsat's temporal extent (1982-present) and spatial resolution (30 m), Landsat 5, 6, 7, and 8 are the best information sources. The time unit to detect conifer and broad-leaved tree distribution change was set at ten-year intervals. Finally, the conifer and broad-leaved tree distribution for 2024 and 2034 were predicted.

3.2 Materials and method

3.2.1 Study flow

To predict the future conifer and broad-leaved tree distributions, three steps were subsequently conducted (Figure 7). At first, forest was classified as being either conifer or broad-leaved tree, using remote sensing. Second, in order to model the replacement probability of conifer by broad-leaved tree, the distribution change of conifer and broad-leaved tree was analyzed. Using analyzed data, the conifer by broad-leaved tree replacement probability was calculated. Finally, the conifer by broad-leaved tree replacement probability was applied to the predicted future distribution of conifer and broad-leaved tree.

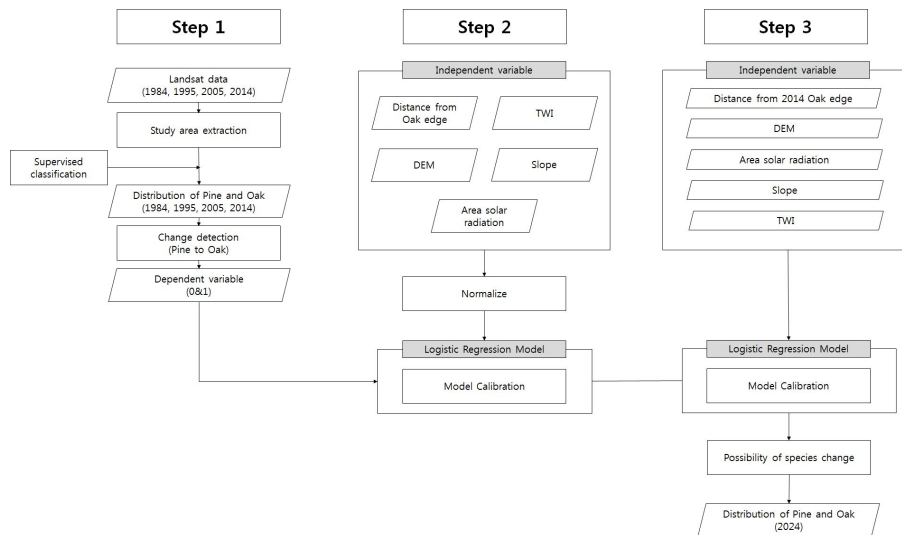


Figure 7. Research flow

3.2.2 Study material

3.2.2.1 Satellite image

In order to calculate the distribution change of conifer and broad-leaved tree, remote sensing data was analyzed. Remote sensing is a tool for collecting data without making physical contact with the object that is studied (Liu and Mason, 2009), and for this study, an optical remote sensing system was used. Optical remote sensing systems measure solar energy reflected from material surfaces (Reddy, 2008), which has great advantages for vegetation analyses (Song and Shin, 2000).

For this study, it was important to consider the successional time scale so that suitable satellite images could be selected. Plant distribution change is a kind of succession. Furthermore, conifer and broad-leaved tree are late successional species, which causes distribution change to occur slowly (Forman and Godron, 1986). Because of these reasons, Landsat images, which have the longest temporal extent, were used.

In addition to time scale, fine scale spatial resolutions increase the power for predicting plant distributions, since plants have relatively short dispersal distances (Guisan et al., 2005). Therefore, this study used Landsat images after 1982 with a 30-m spatial resolution. Furthermore, autumn season images were used, since conifer is an evergreen tree species and broad-leaved tree is deciduous. For this study, the images of November 28, 1984, November 27, 1995, November 22, 2005, November 15, 2014 were used.

3.2.2.2 Variable

The plant species changes from 1984 to 1995, from 1995 to 2005, and from 2005 to 2014 were considered dependent variables. Therefore, analyzed images with the categories 'conifer to broad-leaved tree' and 'conifer to conifer' were generated for the periods 1984-1995, 1995-2005, and 2005-2014 by subtracting the forest cover of 1995 from 1984, of 2005 from 1995, and of 2014 from 2005, respectively (Table 3).

Table 3. Dependent variable for logistic regression

		1984 conifer
1995	conifer	0
	broad-leaved tree	1
		1995 conifer
2005	conifer	0
	broad-leaved tree	1
		2005 conifer
2014	conifer	0
	broad-leaved tree	1

conifer and broad-leaved tree distribution can be affected by elevation, slope, topographic wetness index (TWI), and annual solar radiation (Jung and Kim, 1999; Byun et al., 2010). Therefore, elevation, slope, topographic wetness index (TWI), annual solar radiation, and distance from broad-leaved tree to each cell were considered as independent variables of forest cover change. To calculate annual solar radiation, sum of direct and diffuse radiation of

all sun map and sky map sectors were used. In this calculation, cloud cover was not considered. The result of annual solar radiation indicates that the potential solar radiation of each cell. In this research, annual solar radiation was calculated to modelling the arrived solar radiation for conifer and broad-leaved tree. However, it is hard to predict future cloud cover to calculate annual solar radiation. Therefore, potential solar radiation was used to calculate annual solar radiation. Furthermore, distance from broad-leaved tree to each cell in this study reflects the seed dispersal.

Plant species distribution is in addition determined by soil type and topographic variables (Carlson et al., 2014; Ko et al., 2014). However, soil type data from the past is difficult to collect. In contrast, topographic variables are easy to collect, given their inherent permanence (Brierley and Fryirs, 2008). Therefore, topographic variables that affect plant species distributions were selected for this study (Beier and Brost, 2010).

3.2.3 Method

3.2.3.1 Remote sensing

3.2.3.1.1 Pre-processing

Satellite-collected raw data contains diverse defects and artifacts. It is therefore necessary to pre-process satellite images. Pre-processing generally consists of radiometric corrections, geometric corrections, and atmospheric corrections (Reddy, 2008). Furthermore, to normalize the radiometric characteristics of multiple images through time, topographic correction is important when the research area has rough

terrain (Hantson and Chuvieco, 2011).

This study used level 1 product Landsat images. However, since radiometric and geometric corrections have already been conducted on the Landsat level 1 product, only atmospheric and topographic corrections were conducted here.

Atmospheric corrections were based on a Fast Line-of-Sight Atmospheric Analysis of Spectral Hypercubes (FLAASH) algorithm, and parameters used for this algorithm are listed in table 4.

Table 4. The parameters value used for the FLAASH algorithm

Parameters	Value	Parameters	Value
Solar zenith angle	146.61821305°	Atmosphere model	U.S. Standard
Solar azimuth angle	160.60888483°	Aerosol model	Rural
Latitude	36.03883611°	Water column multiplier	1.00
Longitude	127.76212222°	Visibility	40km

The C-correction method (Teillet et al., 1982), which assumes Lambertian conditions (Civco, 1989), was used to correct for topographic effects. C-correction is considered the best method for vegetation analyses when using Landsat images (Hantson and Chuvieco, 2011).

The first step of the C-correction is calculating the illumination angle, which is based on elevation data. The illumination angle was calculated with the following equation (Equation 1): where γ_i is the incidence angle; θ_s is the solar zenith angle; ϕ_a is the solar azimuth angle; ϕ_s is the slope angle; ϕ_0 is the slope aspect.

$$\cos\gamma_i = \cos(\theta_s)\cos(\eta_i) + \sin(\theta_s)\sin(\eta_i)\cos(\phi_a - \phi_o) \quad \text{Eq. 1}$$

The C-correction was conducted using the following equation (Equation 2, 3): where m_λ is the regression coefficient of illumination; b_λ is the regression constant of band reflectance (Equation 4).

$$\rho_{\lambda,h,i} = \rho_{\lambda,i} \left(\frac{\cos\theta_s + c_\lambda}{\cos\gamma_i + c_\lambda} \right) \quad \text{Eq. 2}$$

$$c_\lambda = \left(\frac{b_\lambda}{m_\lambda} \right) \quad \text{Eq. 3}$$

$$\rho_{\lambda,i} = b_\lambda + m_\lambda \cos\gamma_i \quad \text{Eq. 4}$$

3.2.3.1.2 Image classification and constructing variable

A maximum likelihood classification was performed to classify the vegetation and non-vegetation areas using a Normalized Difference Vegetation Index (NDVI). NDVI is an indicator that represents both the presence and the condition of vegetation, and it is calculated based on following equation (Equation 5): where NIR is the near-infrared band; Red is the red band. Satellite data of Landsat 8 data for 26 May 2014.

$$NDVI = \frac{NIR - Red}{NIR + Red} \quad \text{Eq. 5}$$

The forest area images of 28 November 1984, 27 November 1995, 22 November 2005, and 15 November 2014 were extracted, and

consequently classified into two categories (i.e., conifer or broad-leaved tree). Training data for this classification routine were based on false color composites, for which the interpretation was based on a previous study (Joshi et al., 2014) (Table 5).

Table 5. Interpretation key

	Tone/color	Texture
conifer	Dark red	Smooth
broad-leaved tree	Dark brown	Rough

Maximum likelihood classification was selected from the classification methods. It assumes that the training data for each class are normally distributed, and consequently computes the probability that a given cell belongs to a specific class (Liu and Mason, 2009).

The accuracy of the classified images were assessed. In this research, two kinds of accuracy was assessed which is ROI (region of interest) accuracy and ground truth accuracy. ROI accuracy was computed for all classified images, and ground truth accuracy was computed for 2014 image. Ground truth was performed using Google Earth Pro instead of field survey. Ground truth point was selected by using stratified random sampling method and the number of point was minimum 75 point for each class (Congalton, 1991). Landsat 5 and Landsat 8 images were used in this research. Therefore, classification method for Landsat 5 image was verified using aerial photograph.

Based on these classification results, distribution maps of conifer and broad-leaved tree in 1984, 1995, 2005, and 2014 were constructed. Classes that represented either a 'conifer to broad-leaved tree' or 'conifer to conifer' change were generated for the periods 1984-1995, 1995-2005, and 2005-2014, by subtracting the forest covers of 1995 from 1984, of 2005 from 1995, and of 2014 from 2005, respectively. Here, the dependent variable is binary, with 1 representing 'conifer to broad-leaved tree' and 0 representing 'conifer to conifer'. Observed 'broad-leaved tree to conifer' occurrences were excluded from the dataset, because it was assumed that broad-leaved tree could not be replaced by conifer because of the general successional development (Bae, 1994; Bae and Hong, 1996).

3.2.3.2 Constructing independent variables

The variables elevation, slope, and TWI were based on data from a DEM (digital elevation model). TWI was calculated with the following equation using DEM data (Equation 6): where A_s is the basin area, and β is the slope. In addition, annual solar radiation was computed with the area solar radiation algorithm from ArcGIS. The unit of area solar radiation is watt hours per square meter (WH/m²). The parameters used for the area solar radiation are listed in Table 6. Distance from broad-leaved tree to each cell was measured as the Euclidean distance, using the Euclidean distance algorithm in ArcGIS. In addition, since the time interval was not same among all images, this distance was normalized to 10-year intervals. Finally, collinear

variables were excluded from the dataset, based on correlation analyses, and the units of the variables in the data set were 30m, similar to the Landsat data.

$$TWI = \ln(A_s / \tan\beta) \quad \text{Eq. 6}$$

Table 6. The parameters used for the area solar radiation

Parameters	Value
Day interval	10
Hour interval	0.5

3.2.3.3 Modelling

A logistic regression model was used to analyze the probability of conifer being replaced by broad-leaved tree. The logistic regression model was chosen because it can overcome the limits of linear regression models if the dependent variable has binary values (Sung, 2001; Lee and Kim, 2007).

3.2.3.3.1 Normalize the variable

Independent variables were normalized for a value between 0 and 1, before being included in the logistic regression model. The linear transformation was done for elevation, slope, TWI, and annual solar radiation. Because seed density declines leptokurtically with distance (Nathan and Muller-Landau, 2000; Levey et al., 2008), the inverse proportion of transformation was used for the distance from broad-leaved tree to each cell variable

3.2.3.3.2 Logistic regression

The binary 'conifer to broad-leaved tree' (1) or 'conifer to conifer' (0) was the dependent variable, and elevation, slope, TWI, annual solar radiation, and distance from broad-leaved tree to each cell were the independent variables (Table 7). Data for the period 1984–1995, 1995–2005, and 2005–2014 were integrated for analysis.

Table 7. Variables for logistic regression

Dependent variable	Independent variable
conifer to conifer: 0 conifer to broad-leaved tree: 1	Elevation
	Slope
	TWI
	Annual solar radiation
	Distance from broad-leaved forest edge

To validate the logistic regression model, a relative operating characteristic (ROC) curve and area under curve (AUC) values were generated. AUC values larger than 0.5 imply that a model predicts something better than random assignments of binary data would have. In addition, values between 0.5 and 0.7 are considered low, 0.7–0.9 moderate, and above 0.9 high (Franklin, 2009).

3.2.3.4 Considering uncertainty in distance

Distance from broad-leaved forest edge has uncertainties because of the spatial resolution. For example, figure 8 shows that euclidean distance between adjoining two cells. It calculates the distance between the center of two cell. However, distance from one cell to the other cell is different depends on where the start and end point is (Figure 9).

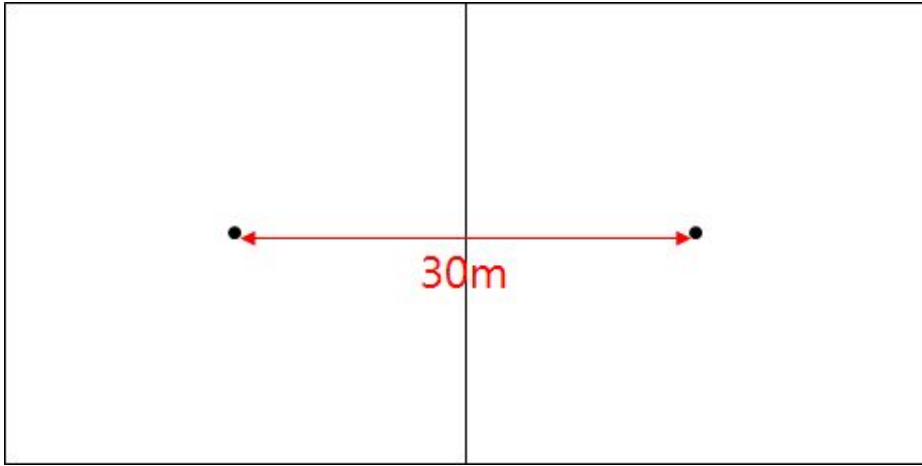


Figure 8. Euclidean distance between two cell

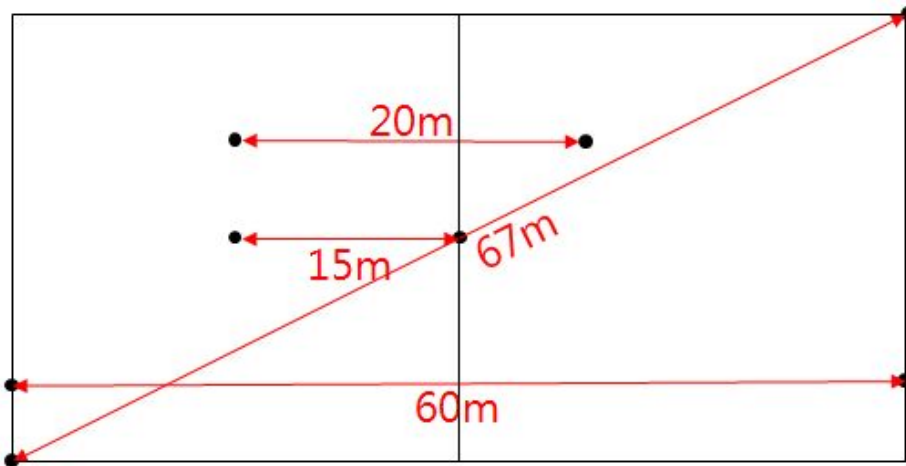


Figure 9. Distance between two cell

A Monte Carlo simulation was conducted to consider uncertainties in distance from broad-leaved forest edge. In order to calculate the distance between two cell, the random point was selected in each cell. In addition, distance between point between each cell was calculated.

Monte Carlo simulation was conducted by using Excel with 20,000 iterations. The algorithm was designed to select the random point in

each cell and to calculate the distance between points. The simulation was performed in all case of distance because standard deviation of simulation result was different in all cases. As a result, the bottom 10%, average, and the top 10% of distance was considered to make logistic regression model.

3.2.3.5 Distribution prediction

The future distribution of conifer and broad-leaved tree was predicted using the logistic regression model. The 2024 distribution was predicted using the conifer and broad-leaved tree distribution map of 2014, whereas the 2034 distribution was predicted with the help of conifer and broad-leaved tree distribution map of 2024.

Table 8. Covered area of conifer and broad-leaved tree

	Area of conifer (km ²)	Area of broad-leaved tree (km ²)	Ratio of conifer (%)	Ratio of broad-leaved tree (%)
1984	137.105	41.593	76.7	23.3
1995	132.409	46.288	74.1	25.9
2005	101.312	77.386	56.7	43.3
2014	70.659	108.038	39.5	60.5

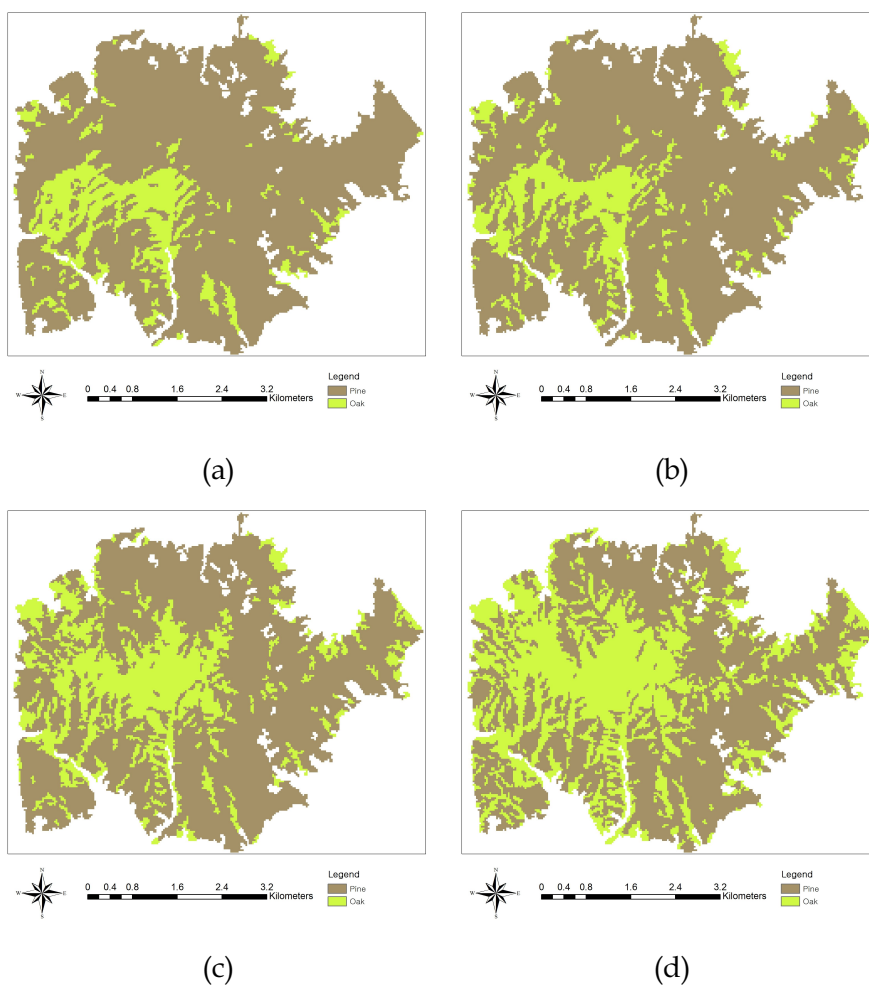


Figure 11. Result of classification. (a) 1984, (b) 1995, (c) 2005, (d) 2014

In case of classified image at 1984, small area was covered by broad-leaved tree at the lower left of forest. It is because broad-leaved tree was good fire wood in contrast with conifer. Therefore broad-leaved tree was logged nearby the human residence which is located at upper left, upper right, lower right (Figure 12). Afforestation was conducted in 1979-1980 around deforested area, using conifer and Japanese alder (*Alnus japonica*). However, Japanese alder was removed after the afforestation because of low economic feasibility. For this reason, it seems that considerable area was suitable for broad-leaved tree but it was planted by conifer. Therefore, it is considered that replacement speed was fast in area that was suitable for broad-leaved tree.

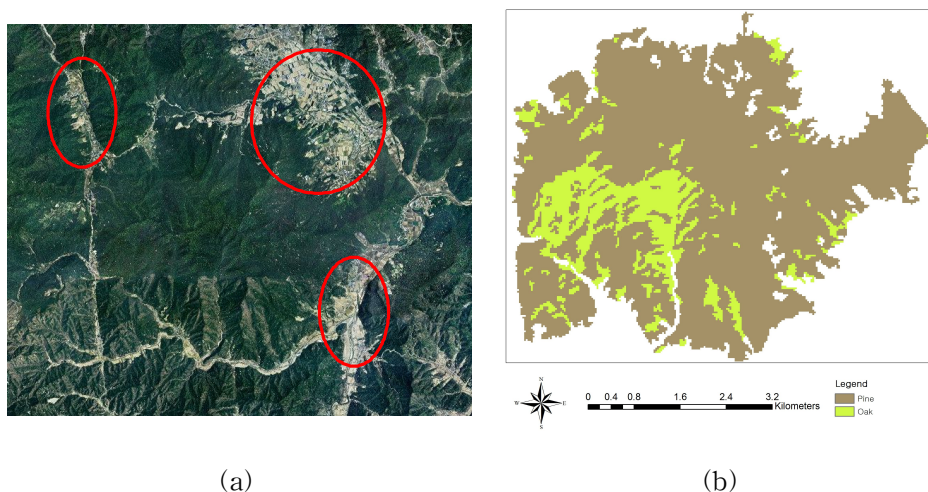


Figure 12. Classification result and residential area. (a) Residential area, (b) Result of classification (1984)

Ratio of conifer was gradually decreased. On the other hand,

broad-leaved tree was gradually increased. In Korea, covered area of pine is most broad in coniferous forest and covered area of *Quercus* spp. is most broad in broadleaf forest (Lim et al., 1995). Pine and *Quercus* spp. are typical species that are in competition (Lee et al., 2006; Byun et al., 2010). Both species are photophilic, which causes them to compete for light (Lee et al., 2006), although pine needs a higher light intensity at its sapling stage (Jung and Kim, 1999). As a result, pine is a weaker competitor compared to *Quercus* spp., and will therefore be replaced by broad-leaved tree under natural conditions (Bae, 1994; Bae and Hong, 1996). In this reason, coniferous forest was decreasing gradually that most coniferous forest is composed of weaker competitor species.

Furthermore, comparing each years covered area, the velocity of increasing ratio of broad-leaved tree was gradually increase. It is considered that the more broad-leaved tree area increase the more velocity of increasing ratio was increased. In addition, It is considered that the more length of contacted surface the more velocity of increasing ratio was increased.

Overall accuracy and kappa coefficient were computed for each image (Table 9). Overall accuracy of every image were over 95%. In general terms, this means that the training set was well selected. In addition, kappa coefficient ,which is over 0.95 for all images, shows that the training set was well selected. As a result of ground truth accuracy assessment for Landsat 8 image, the error matrix was computed (Table 10). Overall accuracy was 85.5% and kappa

coefficient was 0.6997. In general terms, the classified image has substantial agreement (Viera and Garrett, 2005).

Table 9. ROI accuracy and kappa coefficient

Year	Overall accuracy (%)	Kappa coefficient
1984	98.53	0.9606
1995	97.92	0.9577
2005	99.37	0.9875
2014	99.38	0.9852

Table 10. Error matrix for 2014 (Landsat 8)

Classified result	Reference data		Sum	User accuracy
	conifer	broad-leaved tree		
conifer	104	16	120	86.66%
broad-leaved tree	13	67	80	83.75%
Sum	117	83	200	
Producer accuracy	88.88%	80.72%		Overall accuracy = 85.5%

Furthermore, as a result of ground truth accuracy assessment for Landsat 5 image, the error matrix was computed (Table 11). Overall accuracy was 83.5% and kappa coefficient was 0.6584. In general terms, the classified image has substantial agreement (Viera and Garrett, 2005). However, because Landsat 5 has lower technical ability, the accuracy and kappa coefficient value were lower than the result of Landsat 8.

Table 11. Error matrix for 2008 (Landsat 5)

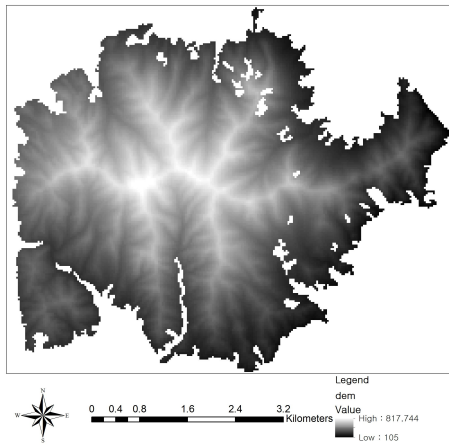
Classified result	Reference data		Sum	User accuracy
	conifer	broad-leaved tree		
conifer	102	18	120	85.00%
broad-leaved tree	15	65	80	81.25%
Sum	117	83	200	
Producer accuracy	87.18%	78.31%		Overall accuracy = 83.5%

4.2 Logistic regression

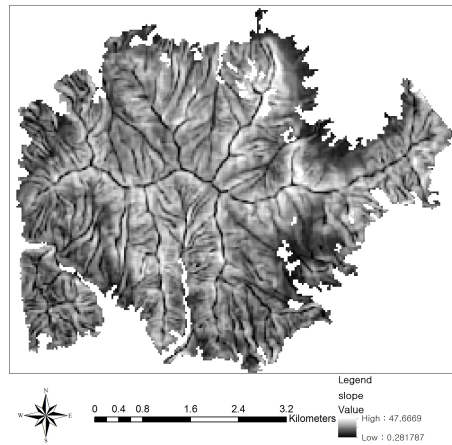
4.2.1 Constructing variable

Analyzed map with the categories ‘conifer to broad-leaved tree’ and ‘conifer to conifer’ were generated for the period 1984–1995, 1995–2005 and 2005–2014. To conduct logistic regression categories were converted into binary ‘conifer to broad-leaved tree’ or ‘conifer to conifer’, where 1=‘conifer to broad-leaved tree’ and 0=‘conifer to conifer’.

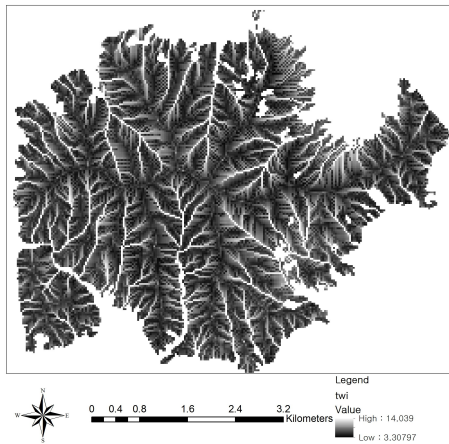
Elevation, slope, TWI, annual solar radiation were made based on DEM data (Figure 13). Variables were normalized between 0 and 1 before including in the logistic regression model. Furthermore, distance from broad-leaved forest edge was computed at each year (Figure 14).



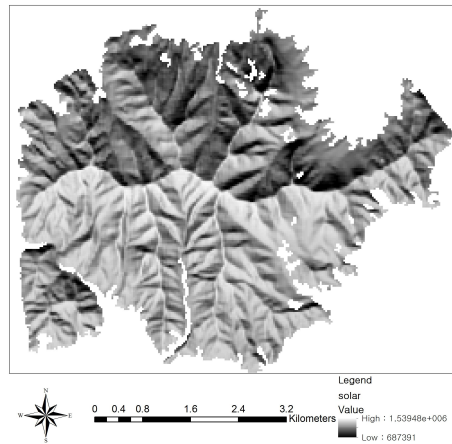
(a)



(b)



(c)



(d)

Figure 13. Independent variables. (a) Elevation, (b) Slope, (c) TWI, (d) Annual solar radiation

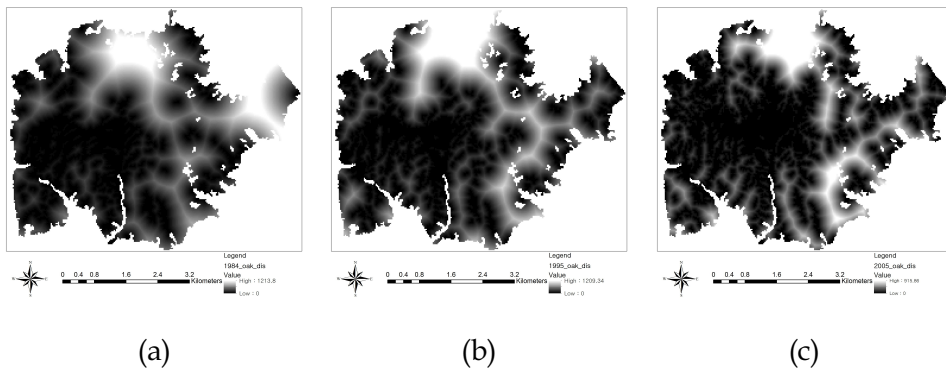


Figure 14. Distance from broad-leaved forest edge. (a) 1984, (b) 1995, (c) 2005

Distance from broad-leaved forest edge was normalized considering relationship between distance and replaced ratio of conifer by broad-leaved tree. As a result of frequency analysis, 90% of replaced cell was existed within 241m (Table 12). Through this result, it is considered that distance of the sapling from the parent individual has relationship with seed dispersal ability (Nathan and Muller-Landau, 2000; Levey et al., 2008), because the trend of sapling density appears similar to seed density. Furthermore, the effect of dispersal ability on broad-leaved tree are similar to those of *Quercus macrocarpa* (Dow and Ashley, 1996). Number of *Quercus macrocarpa* sapling was sharply decreased depends on distance, similar with the relust of this research.

Table 12. Statistical result of frequency analysis

	Value
Average	91.58
Skewness	3.893
Kurtosis	23.116
Top 90%	241

If distance from broad-leaved forest edge is over 241m, it is considered that replacement probability of conifer by broad-leaved tree is very low. Therefore, logistic regression was conducted using data distance from broad-leaved forest edge is within 241m.

Dispersal of broad-leaved tree seed was conducted by wildlife such as Siberian chipmunks (*Tamias sibiricusbarberi*), Korean squirrel (*Sciurus vulgariscoreae*) Wild boar (*Sus scrofa*) (Kim and Kim, 2013). Considering the home range as circle, radius of home range of Siberian chipmunks is 200m (Jo et al., 2014), Eurasian red squirrel is 45-140m (Flyger, 1960), Wild boar is 280-330m (Russo et al., 1997). Therefore, it is adequate that the replacement was occurred near 241m from broad-leaved forest edge.

To figure out the relationship between replacement ratio and distance from broad-leaved forest edge, curve estimation was conducted. The R^2 of the inverse function is 0.923, therefore, inverse function is turn out to be most suitable (Figure 15). According to this result, inverse proportion transformation was conducted for distance from broad-leaved forest edge.

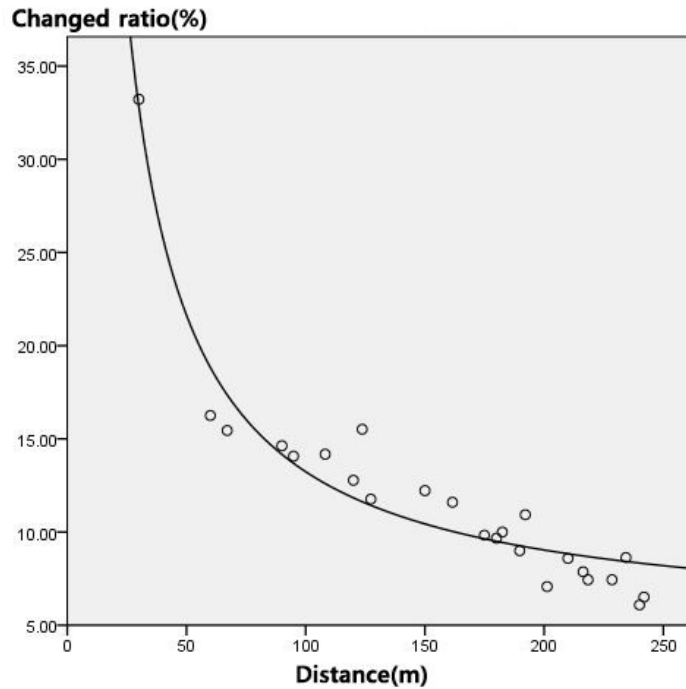


Figure 15. Graph of replacement ratio and distance from broad-leaved forest edge

4.2.2 Logistic regression model

To make logistic regression model, data for period 1984–1995, 1995–2005 and 2005–2014 were integrated. For dependent variable, the binary ‘conifer to broad-leaved tree’ and ‘conifer to conifer’ was used. Correlation analysis was used to exclude highly correlated variables that correlation coefficient over ± 0.6 (Table 13). The highest value was appeared in twi which is -0.428 , however, value is lower than 0.6. Therefore, all independent variables were used to make logistic regression.

Table 13. Result of correlation coefficient analysis

		Distance	Annual solar radiation	Elevation	Slope	TWI
Distance	Pearson correlation	1	-.075**	-.145**	-.021**	0.48**
	P-value		0.000	0.000	0.000	0.000
Annual solar radiation	Pearson correlation	-.075**	1	-.070**	-.386**	.058**
	P-value	0.000		0.000	0.000	0.000
Elevation	Pearson correlation	-.145**	-.070**	1	.288**	-.185**
	P-value	0.000	0.000		0.000	0.000
Slope	Pearson correlation	-.021**	-.386**	.288**	1	-.428**
	P-value	0.000	0.000	0.000		0.000
TWI	Pearson correlation	.048**	.058**	-.185**	-.428**	1
	P-value	0.000	0.000	0.000	0.000	

** . P<0.05

Table 14 and 15 show the result of logistic regression model. All independent variables were selected in logistic regression model, because p value of independent variables were less than 0.05. Therefore, Equation 7 is developed logistic regression model: where X_1 is the elevation, X_2 is the slope, X_3 is the TWI, X_4 is the annual solar radiation, X_5 is the distance from broad-leaved forest edge.

Table 14. Result of logistic regression analysis

	B	S.E	df	p
Elevation	1.924	0.065	1	0.000
Slope	-0.710	0.102	1	0.000
TWI	1.617	0.100	1	0.000
Annual solar radiation	-3.443	0.075	1	0.000
Distance from broad-leaved tree ti each cell	-2.043	0.039	1	0.000
Intercept	1.089	0.096	1	0.000

Table 15. statistics of logistic regression model

Model statistics	Value
R-square	0.195
AUC/ROC	0.752

$$\text{Logit}(p) = 1.089 + 1.924X_1 - 0.710X_2 + 1.617X_3 - 3.443X_4 - 2.043X_5 \quad \text{Eq. 7}$$

Among the variables, annual solar radiation was the best predictor for replacement probability of conifer by broad-leaved tree, with a B value of -3.209. This means that the replacement probability of conifer by broad-leaved tree increases where total amount of solar radiation is large. It is because seed of conifer needs more solar radiation than broad-leaved tree to sprout (Jung and Kim, 1999). Furthermore, it is similar to result of site-scale process that shade tolerance and seed dispersal ability are turn out to important factor (Liang et al., 2015).

distance from broad-leaved forest edge was the secondarily important predictor, with a B value of -2.166. This means that the

replacement probability of conifer by broad-leaved tree increases near the broad-leaved forest edges than away from broad-leaved forest edges. It is because probability of long distance seed dispersal is low and seed density declines sharply with distance. In addition, it is considered that seed dispersal determine the establishment and exist of the individual (Levin et al., 2003; Levey et al., 2008).

The accuracy estimate of distribution of conifer and broad-leaved tree map is shown in Table 16. The logistic regression model was having accuracy of 83.0%. ROC graph was generated between model predicted distribution of conifer and broad-leaved tree and the actual distribution is shown in Figure 16. AUC value was 0.759 which means normal suitability.

Table 16. Error matrix of logistic regression model

True category	Predicted category		Accuracy(%)
	Not change	Change	
Not change	39044	886	97.8
Change	7566	1254	14.2
Overall			82.7

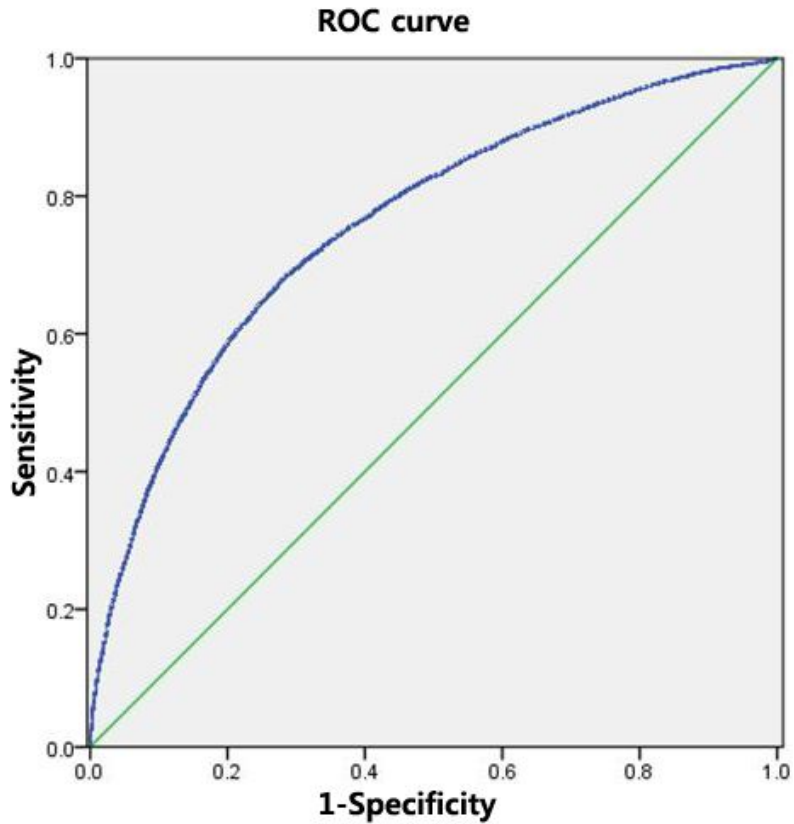


Figure 16. ROC curve

4.2.3 Considering uncertainty

As a result of simulation the variation of distance was calculated. For example, in case of adjoining two cell, histogram was shown in figure 17. Calculated distance in ArcGIS using euclidean distance was 30m, however, according to simulation, average distance is 32.73m.

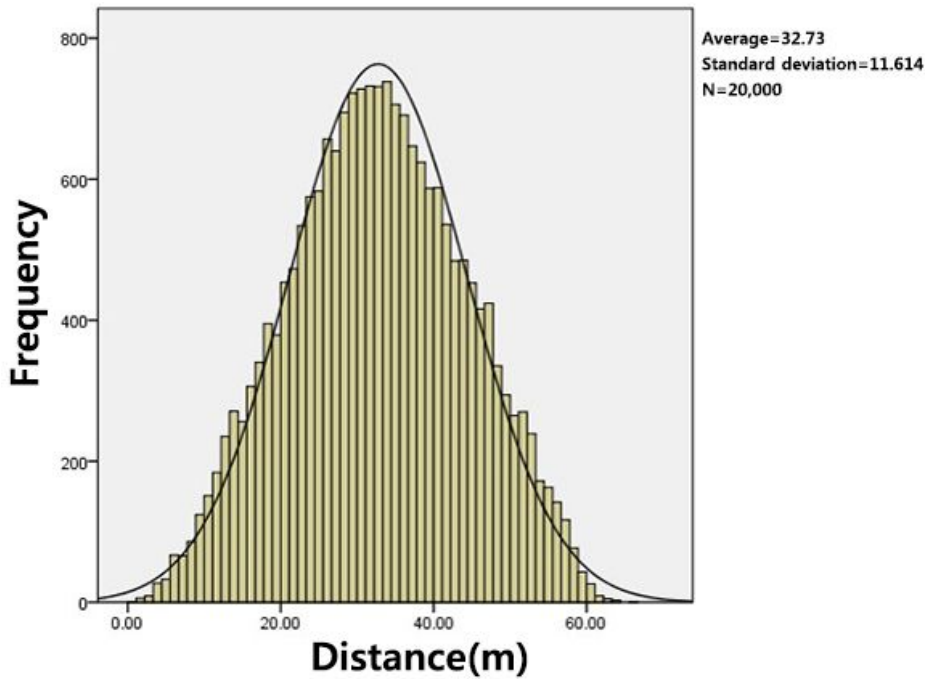


Figure 17. Histogram of simulation

To consider the variation of distance from broad-leaved forest edge, the result of Monte Carlo simulation was classified into 3 cases: bottom 10%; average; top 10% (Appendix. Table S-1). Table 17, 18, 19 shows the result of logistic regression model for all cases: bottom 10%=model A, average=model B, top10%=model C. B value of distance from broad-leaved forest edge was different at three cases. Furthermore, as B value of distance from broad-leaved forest edge was decreased the other variables B value was increased.

Table 17. Result of logistic regression analysis (model A)

	B	S.E	df	p
Elevation	1.939	0.066	1	0.000
Slope	-0.732	0.102	1	0.000
TWI	1.601	0.100	1	0.000
Annual solar radiation	-3.445	0.075	1	0.000
Distance from broad-leaved tree to each cell	-1.999	0.037	1	0.000
Intercept	1.130	0.096	1	0.000

Table 18. Result of logistic regression analysis (model B)

	B	S.E	df	p
Elevation	1.914	0.065	1	0.000
Slope	-0.694	0.102	1	0.000
TWI	1.626	0.100	1	0.000
Annual solar radiation	-3.442	0.075	1	0.000
Distance from broad-leaved tree to each cell	-2.067	0.040	1	0.000
Intercept	1.056	0.095	1	0.000

Table 19. Result of logistic regression analysis (model C)

	B	S.E	df	p
Elevation	1.903	0.065	1	0.000
Slope	-0.666	0.101	1	0.000
TWI	1.639	0.100	1	0.000
Annual solar radiation	-3.422	0.075	1	0.000
Distance from broad-leaved tree to each cell	-2.090	0.042	1	0.000
Intercept	0.978	0.095	1	0.000

4.2.4 Distribution prediction

Predicted distribution was shown in figure 18, 19. 2024 distribution of conifer and broad-leaved tree was predicted based on 2014

distribution, and 2034 was predicted based on predicted 2024 distribution.

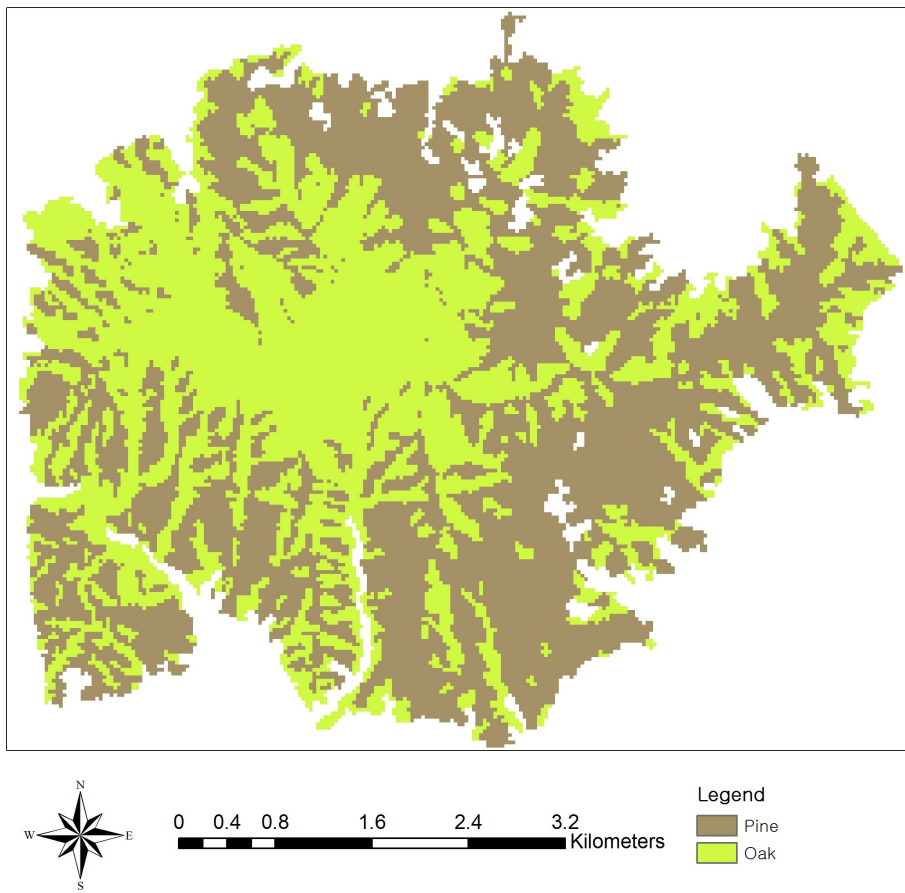


Figure 18. Predicted distribution at 2024

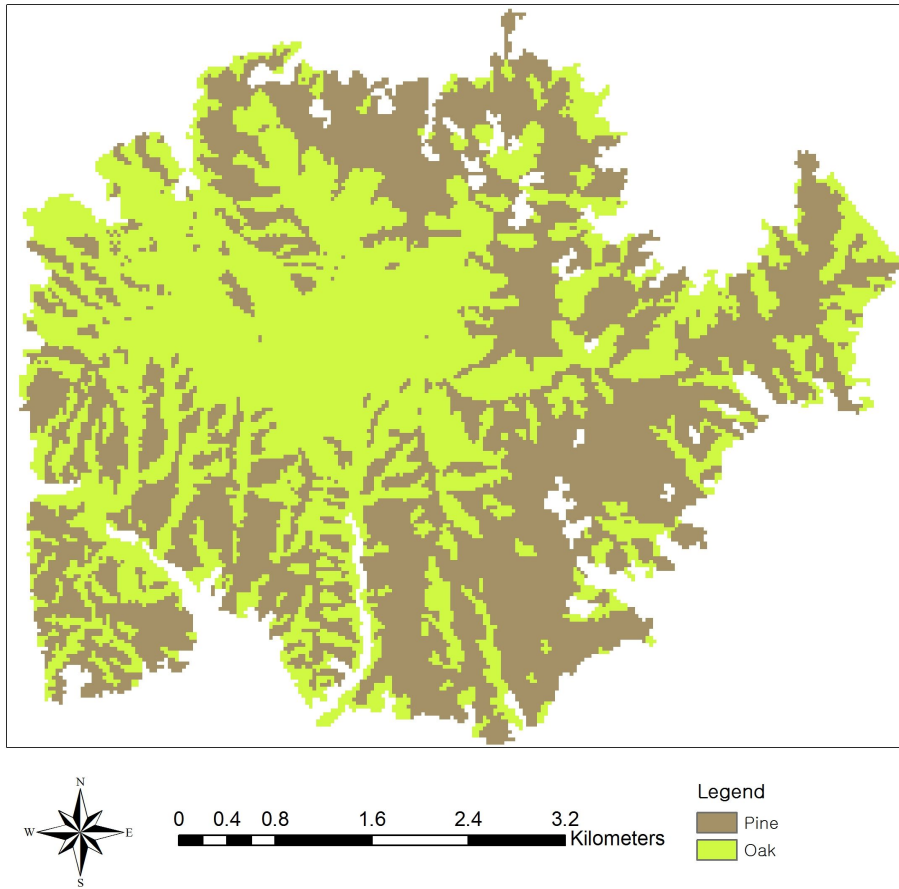


Figure 19. Predicted distribution at 2034

Covered area of conifer and broad-leaved tree was calculated from past to future. Covered area of conifer decrease over time, especially at 1995 to 2014 (Figure 20). In contrast, replacement of conifer by broad-leaved tree was decreased at 2024 to 2034. It is considered that there are small suitable area for broad-leaved tree because suitable area was decreased continuously. Therefore, replacement of conifer by broad-leaved tree seems to decrease continuously.

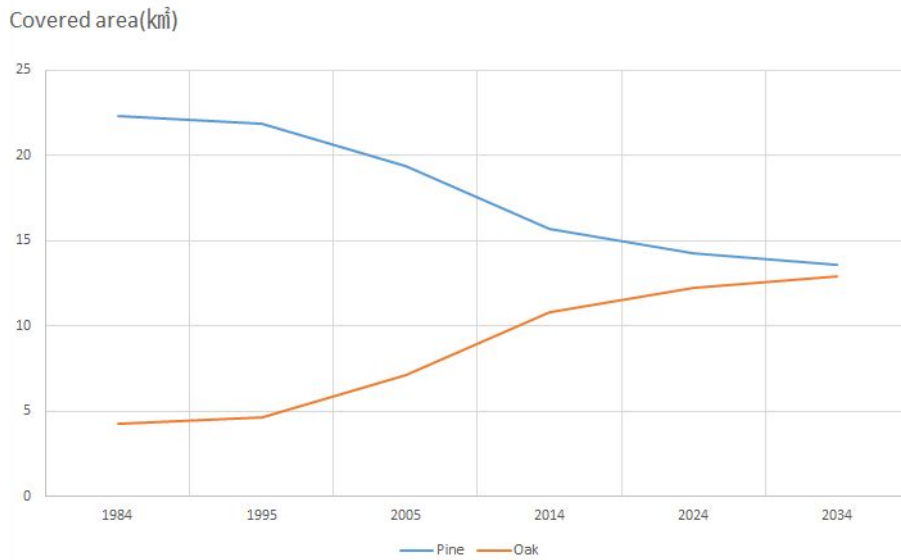


Figure 20. Covered area change of conifer and broad-leaved tree

In addition, graph of covered area of broad-leaved tree is similar to that of population growth. broad-leaved tree population curve seems similar to sigmoid curve which known as population growth model (Ryu and Lee, 2002). It is considered that forest area comes to limited resource, therefore, competition was occurred between conifer and broad-leaved tree.

4.2.5 Distribution prediction considering uncertainty in distance

Distribution prediction considering uncertainty was conducted based on three logistic model: model A, model B, model C (Appendix Figure S-2). Predicted covered area was shown in Table 20 and Figure 21.

In case of 2014 to 2024, covered area of conifer was decreased 1.52km² (model A), 1.36km² (model B), 1.24km² (model C). Furthermore, in case of 2024 to 2034, covered area of conifer was decreased 0.71km² (model A), 0.63km² (model B), 0.56km² (model C). Covered area of conifer was decreased faster when applying model A. That is because the model A is more sensitive to distance. In addition, replacement speed of model A was most fast. Compare to model A, model B was 10% point slower and model C was 10% slower.

Table 20. Predicted covered for each model

	2024		2034	
	conifer (km ²)	broad-leaved tree (km ²)	conifer (km ²)	broad-leaved tree (km ²)
Model A	14.1624	12.3291	13.4460	13.0455
Model B	14.3208	12.1707	13.6827	12.8088
Model C	14.4369	12.0546	13.8672	12.6243

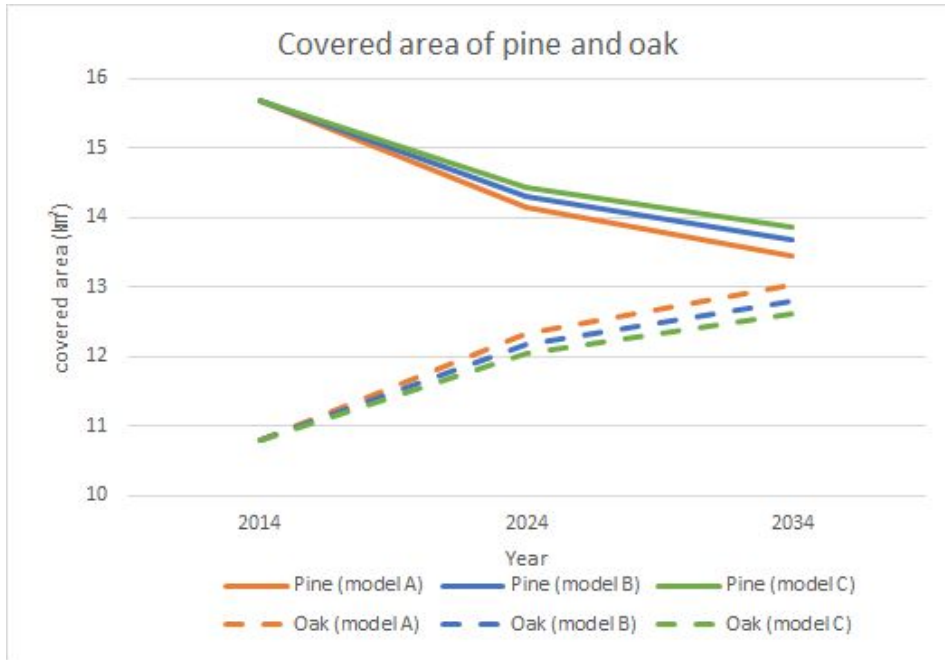


Figure 21. Covered area of conifer and broad-leaved tree

5. Conclusion

In this research, distribution of conifer and broad-leaved tree at Namsan (Mt.) were analyzed and future distributions of conifer and broad-leaved tree at Namsan (Mt.) were predicted. Remote sensing was used to make past distribution of conifer and broad-leaved tree. Satellite data was useful to classify conifer and broad-leaved tree, and suitable for obtain past data.

As a result of classification, it is considered that distribution of conifer and broad-leaved tree at Namsan in 1984 was highly affected by human activity which is heating because afforestation was done in 1979–1980 where broad-leaved trees were deforested for fire wood. Furthermore, speed of distribution change was fast. It is considered that Namsan was suitable for broad-leaved tree, however it was afforested by conifers.

In addition, in this research, replacement probability of conifer by broad-leaved tree and present distribution of conifer and broad-leaved tree was used to predict future distribution of conifer and broad-leaved tree. In addition to environmental variables which is commonly used in other researches, distance from broad-leaved forest edge was used. Distance variable reflects distribution changing process because seed density is highly affected by distance and plant species distribution is highly affected by species distribution. Furthermore, the scale of data is flexible using GIS tools. However, spatial and temporal resolution is limitation of the data. To overcome limitation of spatial resolution, Monte Carlo simulation was used. In

addition, to overcome the limitation of temporal resolution, distance variable was normalized to 10-year intervals.

As a result, annual solar radiation and distance from broad-leaved forest edge was turn out to be an important variable to predict replacement probability of conifer by broad-leaved tree. Most replacement was occurred near the broad-leaved tree and as the distance from broad-leaved forest edge increases, the replacement was decreased. This result indicates that the distance is suitable variable to predict future distribution and to reflect seed dispersal ability.

Trends of distribution change from past to present, changes in the recent distribution is larger than past. According to this result, it seems that conifer will disappear shortly in research area. In contrast, according to result of future prediction, distribution changes were smaller than current change. It indicates that suitable area for broad-leaved tree is decreasing.

Because researches using dispersal ability and more than two species in high resolution at large scale is poor, this study selected two species that relationship between species are clear and studied well. However, areas that inhabit two species are scarce so that it is hard applicate this method. Therefore, to use the result for forest management, researches that consider more than two species are need. Furthermore, relationship between conifer and broad-leaved tree is very clear and simple, however, there are more species interactions that this research cannot consider.

Types or conditions of soil is important variable to predict plant distribution. However it doesn't considered in this research because it is impossible to obtain or construct past and future state. In spite of this limitation, logistic regression model made in this research predict distribution properly. In addition, disturbances were not considered in this research. Therefore, distribution change in this research reflects natural process excluding disturbance.

6. References

- Bae, K., & Hong, S. (1996). Structure and Dynamics of *Pinus densiflora* Community in Mt. Kaya. *Journal of Korean Forest Society*, 85(2), 260-270.
- Bae, S. (1994). Structure and Tending Method for Naturally Regenerated Young *Pinus Densiflora* Sieb . et Zucc . Stands, *Journal of Korean Forest Society*, 83(1), 50-62
- Beale, C. M., & Lennon, J. J. (2012). Incorporating uncertainty in predictive species distribution modelling. *Philosophical Transactions of the Royal Society B: Biological Sciences*, 367(1586), 247 - 258. doi:10.1098/rstb.2011.0178
- Brierley, G., & Fryirs, K. (2008). *Geomorphology and river management: applications of the river styles framework*. Wiley-Blackwell.
- Brost, B. M. & Paul, B (2015). Use of land facets to design linkages for climate change. *Ecological Applications*, 22(1), 87 - 103.
- Byun, J., Lee, W., Nor, D., Kim, S., Choi, J., & Lee, Y. (2010). The Relationship Between Tree Radial Growth and Topographic and Climatic Factors in Red conifer and broad-leaved tree in Central Regions of Korea. *Journal of Korean Forest Society*, 99(6), 908-913.
- Carlson, B., Wang, D., Capen, D., & Thompson, E. (2004). An evaluation of GIS-derived landscape diversity units to guide landscape-level mapping of natural communities. *Journal for Nature Conservation*, 12(1), 15 - 23. doi:10.1016/j.jnc.2003.07.001
- Choi, S., Lee, W., Kwak, D., Lee, S., Son, Y., Lim, J., & Saborowski, J. (2011). Predicting forest cover changes in future climate using hydrological and thermal indices in South Korea. *Climate Research*, 49(3), 229 - 245. doi:10.3354/cr01026
- Clark, J. S., Silman, M., Kern, R., Macklin, E., & Hillerislambers, J. (2010). Seed Dispersal near and Far : Patterns across Temperate and

Tropical Forests Published by : Ecological Society of America
SEED DISPERSAL NEAR AND FAR : PATTERNS ACROSS
TEMPERATE AND TROPICAL FORESTS (I ~, 80(5), 1475 -
1494.

- Congalton, R. G. (1991). A review of assessing the accuracy of classifications of remotely sensed data. *Remote Sensing of Environment*, 37(1), 35 - 46. doi:10.1016/0034-4257(91)90048-B
- Defries, R. S., & Townshend, J. R. G. (1994). NDVI-derived land cover classifications at a global scale. *International Journal of Remote Sensing*, 15(17), 3567 - 3586. Retrieved from <http://www.scopus.com/inward/record.url?eid=2-s2.0-0028582679&partnerID=40&md5=03abfa9cce34b995703cdf7542023d4>
- Dow, B. D. and M. V. A. (n.d.). (1996). Microsatellite analysis of seed dispersal and parentage of saplings in bur broad-leaved tree. *Molecular Ecology*, 5, 615-627.
- Flyger, V.F. (1960). Movement and home range of the gray squirrel, *Sciurus carolinensis*, in two Maryland Woodlot., *Ecology* 41, 365-369.
- Forman, R. T. T. & Godron M. (1986). *Landscape ecology*. New York; John Wiley & Sons.
- Franklin, J. (2009). *Mapping species distributions*. Cambridge university press.
- Ge, J., Xiong, G., Zhao, C., Shen, G., & Xie, Z. (2013). Forest Ecology and Management Short-term dynamic shifts in woody plants in a montane mixed evergreen and deciduous broadleaved forest in central China. *Forest Ecology and Management*, 310, 740 - 746. doi:10.1016/j.foreco.2013.09.019
- Guisan, A., & Thuiller, W. (2005). Predicting species distribution: Offering more than simple habitat models. *Ecology Letters*, 8(9), 993 - 1009. doi:10.1111/j.1461-0248.2005.00792.x

- Hantson, S., & Chuvieco, E. (2011). Evaluation of different topographic correction methods for landsat imagery. *International Journal of Applied Earth Observation and Geoinformation*, 13(5), 691 - 700. doi:10.1016/j.jag.2011.05.001
- Huang, C.Q., Kim, S., Song, K., Townshend, J.R.G., Davis, P., Altstatt, A., Rodas, O., Yanosky, A., Clay, R., Tucker, C.J., Musinsky, J., 2009. Assessment of Paraguay's forest cover change using Landsat observations. *Glob. Planet. Change* 67, 112.
- Jia, K., Liang, S., Zhang, L., Wei, X., Yao, Y., & Xie, X. (2014). Forest cover classification using Landsat ETM+ data and time series MODIS NDVI data. *International Journal of Applied Earth Observation and Geoinformation*, 33(1), 32 - 38. doi:10.1016/j.jag.2014.04.015
- Jönsson, P., & Eklundh, L. (2002). Seasonality extraction by function fitting to time-series of satellite sensor data. *IEEE Transactions on Geoscience and Remote Sensing*, 40(8), 1824 - 1832. doi:10.1109/TGRS.2002.802519
- Jo, Y.S., Hong, S., John, T.B. (2014). Habitat and food utilization of the Siberian chipmunk, *Tamias sibiricus*, in Korea. *Acta Theriol*, 59, 589-594.
- Joshi, a. K., Joshi, P. K., Chauhan, T., & Bairwa, B. (2014). Integrated approach for understanding spatio-temporal changes in forest resource distribution in the central Himalaya. *Journal of Forestry Research*, 25(2), 281 - 290. doi:10.1007/s11676-014-0459-9
- Jung, D., & Kim, Y. (1999). A Study on Light Condition between *Pinus densiflora* and *Quercus variabilis* Natural Mixed Forest Stands by Using the Hemispherical Photo Method. *Korean Journal of Agricultural and Forest Meteorology*, 1(2), 127-134.
- Kim, D., Sexton, J. O., Noojipady, P., Huang, C., Anand, A., Channan, S.,

- Feng, M., Townshend, J. R. (2014). Remote Sensing of Environment Global, Landsat-based forest-cover change from 1990 to 2000. *Remote Sensing of Environment*, 155, 178 - 193. doi:10.1016/j.rse.2014.08.017
- Kim, G.T., Kim, H.J. (2013). Secondary Dispersion of Several Broadleaved Tree Seeds by Wildlife in Mt. Jungwang, Pyeongchang gun, Korea. *Korean Journal of Environment Ecology*, 27(1), 64-70.
- Ko, S., Sung, J., Chun, J., Lee, Y., & Shin, M. (2014). Predicting the Changes of Yearly Productive Area Distribution for *Pinus densiflora* in Korea Based on Climate Change Scenarios. *Korean Journal of Agricultural and Forest Meteorology*, 16(1), 72-82. doi:10.5532/KJAFM.2014.16.1.72
- Kwak, D.-A., Lee, W.-K., Son, Y., Choi, S., Yoo, S., Chung, D. J., Lee, S.-H., Kim, S.H., Choi J.K., Lee, Y.J. & Byun, W.-H. (2012). Predicting distributional change of forest cover and volume in future climate of South Korea. *Forest Science and Technology*, 8(2), 105 - 115. doi:10.1080/21580103.2012.673751
- Lee, D., & Kim, J. (2007). Vulnerability Assessment of Sub-Alconifer Vegetations by Climate Change in Korea. *Journal of Environmental Resources & Revegetation Technology* , 10(6), 110-119.
- Lee, J., Lee, W., Yoon, J., & Song, C. (2006). Distribution Pattern of *Pinus densiflora* and *Quercus* Spp. Stand in Korea Using Spatial Statistics and GIS . *Journal of Korean Forest Society*, 95(6), 663-671.
- Leinenkugel, P., Wolters, M. L., Oppelt, N., & Kuenzer, C. (2015). Tree cover and forest cover dynamics in the Mekong Basin from 2001 to 2011. *Remote Sensing of Environment*, 158, 376 - 392. doi:10.1016/j.rse.2014.10.021
- Levey, D. J., Tewksbury, J. J., & Bolker, B. M. (2008). Modelling

- long-distance seed dispersal in heterogeneous landscapes. *Journal of Ecology*, 96(4), 599 - 608. doi:10.1111/j.1365-2745.2008.01401.x
- Levin, S. a., Muller-Landau, *Helene C., Nathan, *Ran, & Chave, *Jérôme. (2003). The Ecology and Evolution of Seed Dispersal: A Theoretical Perspective. *Annual Review of Ecology, Evolution, and Systematics*, 34(1), 575 - 604. doi:10.1146/annurev.ecolsys.34.011802.132428
- Liang, Y., He, H. S., Wang, W. J., Fraser, J. S., Wu, Z., & Xu, J. (2015). The site-scale processes affect species distribution predictions of forest landscape models. *Ecological Modelling*, 300, 89 - 101. doi:10.1016/j.ecolmodel.2015.01.007
- Liu, J. G., & Mason, P. (2009). *Essential Image Processing and GIS for Remote Sensing*. WILEY-BLACKWELL. <http://ezproxy.utwente.nl:2163/patron/FullRecord.aspx?p=454358>
- Michael, L. Cain, Brook, G. Milligan, A. A. E. S. (2000). Long-Distance Seed Dispersal in Plant Populations. *American Journal of Botany*, 87(9), 1217 - 1227. doi:10.1016/j.tree.2011.08.009
- Moorcroft, P. R., Hurtt, G. C., & Pacala, S. W. (2001). A method for scaling vegetation dynamics: The ecosystem demography model (ED). *Ecological Monographs*, 71(4), 557 - 586. doi:10.1890/0012-9615(2001)071[0557:AMFSVD]2.0.CO;2
- Muraoka, H., Saitoh, T.M. and Nagai, S., 2015. Long-term and interdisciplinary research on forest ecosystem functions : challenges at Takayama site since 1993 Takayama chronicle. pp.197?200.
- Nathan, R., & Muller-Landau, H. C. (2000). Spatial patterns of seed dispersal, their determinants and consequences for recruitment. *Trends in Ecology and Evolution*, 15(7), 278 - 285. doi:10.1016/S0169-5347(00)01874-7
- Ohmann, J. L., Gregory, M. J., Roberts, H. M., Cohen, W. B., Kennedy, R. E., Yang, Z. (2012) Mapping change of older forest with

- nearest-neighbor imputation and Landsat time-series, *Forest Ecology and Management*, 272, 13-25.
- Pacala, S. W. (1986). Neighborhood Models of Plant Population Dynamics. 4. Single-Species and Multispecies Models of Annuals with Dormant Seeds. *The American Naturalist*, 128(6), 859. doi:10.1086/284610
- Park, H., Hyun, C., & Oh, S. (2011). *Remote Sensing for Energy Resources*. CIR press.
- Pettorelli, N., Vik, J. O., Mysterud, A., Gaillard, J. M., Tucker, C. J., & Stenseth, N. C. (2005). Using the satellite-derived NDVI to assess ecological responses to environmental change. *Trends in Ecology and Evolution*, 20(9), 503 - 510. doi:10.1016/j.tree.2005.05.011
- Reddy, M. A. (2008). *Remote sensing and geographical information systems*. BS Publications
- Russo, L., Massei, G. Genov P. V. (1997). Daily home range and activity of wild boar in a mediterranean area free from hunting. *Ethology Ecology & Evolution*, 9(3), 287-294.
- Ryu, M., & Lee, J., (2002). *Population Ecology*. SNU press.
- Sexton, J.O., Song, X.-P., Huang, C., Channan, S., Baker, M.E., Townshend, J.R. (2013). Urban growth of the Washington, D.C. Baltimore,MDmetropolitan region from 1984 to 2010 by annual, Landsat-based estimates of impervious cover. *Rem. Sens. Environ.* 129, 4253.
- Song, C., A. Schroeder, T., B. Cohen, W. (2007) Predicting temperate conifer forest successional stage distributions with multitemporal Landsat Thematic Mapper imagery. *Remote Sensing of Environment*, 106, 228-237.
- Song, D.-X., Huang, C., Sexton, J. O., Channan, S., Feng, M., & Townshend, J. R. (2015). Use of Landsat and Corona data for mapping forest cover change from the mid-1960s to 2000s: Case studies from the

- Eastern United States and Central Brazil. *ISPRS Journal of Photogrammetry and Remote Sensing*, 103, 81 - 92. doi:10.1016/j.isprsjprs.2014.09.005
- Song, M., & Shin, K. (2000). Variation Analysis of Forest Resources in Anmyundo Using Landsat TM . *Journal of Korean Earth Science Society*, 21(2), 188-200.
- Song, W., & Kim, E. (2012). A Comparison of Machine Learning Species Distribution Methods for Habitat Analysis of the Korea Water Deer (*Hydropotes inermis argyropus*). *Korean Journal of Remote Sensing*, 28(1), 171 - 180. doi:10.7780/kjrs.2012.28.1.171
- Sung, W. (2001). *Applied Logistic Regression Analysis- Theory, Methods, SAS Applications*. Seoun Tamjin
- Suzuki, R., Nomaki, T., & Yasunari, T. (2001). Spatial distribution and its seasonality of satellite-derived vegetation index (NDVI) and climate in Siberia. *International Journal of Climatology*, 21(11), 1321 - 1335. doi:10.1002/joc.653
- Teillet, P. M., Guindon, B., & Goodenough, D. G. (1981). On the Slope-Aspect Correction of Multispectral Scanner Data Seventh International Symposium Machine Processing of Remotely Sensed Data, (July). doi:10.1080/07038992.1982.10855028
- Tilman, D. & Kareiva, P. (1997) *Spatial ecology*. Princeton university press.
- van der Marrel, E., Franklin, J. (2013) *Vegetation Ecology*. John Wiley & Sons
- Viera, A. J., & Garrett, J. M. (2005). Understanding interobserver agreement: The kappa statistic. *Family Medicine*, 37(5), 360 - 363. doi:Vol. 37, No. 5
- Willson, M.F. (1992). The ecology of seed dispersal. M. Fenner (Ed.), *Seeds: The Ecology of Regeneration in Plant Communities*, CAB International (1992), pp. 61 - 85

7. Appendix

Table S-1. Result of Monte Carlo simulation

Euclidean distance (m)	Simulation result			
	Bottom 10% (m)	Average (m)	Top 10% (m)	Standard deviation
30.00	17.25	32.57	48.24	11.61396
42.42	28.54	44.16	59.79	12.00784
60.00	44.91	61.08	77.49	12.15693
67.08	52.21	68.15	84.02	12.07155
84.85	69.58	85.66	101.59	12.18375
90.00	74.41	90.69	107.12	12.21235
94.86	79.58	95.67	111.8	12.18882
108.16	92.90	108.81	124.79	12.21335
120.00	104.16	120.51	136.9	12.19706
123.69	108.16	124.34	140.82	12.12031
127.27	111.82	127.76	143.51	12.32026
134.16	118.68	134.70	150.75	12.20274
150.00	133.94	150.33	166.72	12.24262
152.97	137.16	153.44	169.92	12.0856
161.55	145.93	161.91	178.19	12.16194
169.70	154.24	170.13	185.87	12.23276
174.92	159.37	175.17	191.36	12.21164
180.00	163.92	180.47	197.17	12.25031
182.48	166.37	183.12	199.68	12.20302
189.73	173.75	190.27	206.49	12.25554
192.09	176.52	192.39	208.36	12.15541
201.24	185.64	201.67	218.00	12.22688
210.00	193.75	210.27	226.72	12.24445
212.13	196.01	212.56	228.95	12.20369
216.33	200.58	216.83	232.66	12.1515
218.40	202.54	218.71	235.15	12.22148
228.47	212.50	228.67	244.93	12.22148
234.30	218.59	234.87	251.04	12.24937
240.00	223.63	240.29	257.09	12.3069
241.86	225.56	242.31	258.96	12.28898



(a)



(b)



(c)



(d)



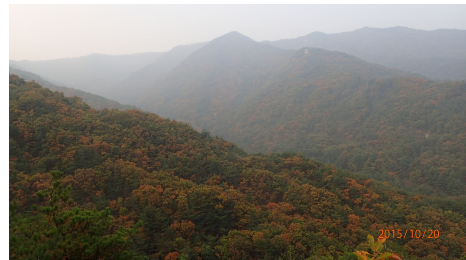
(e)



(f)

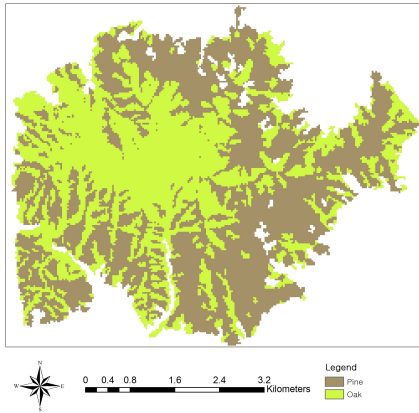


(g)

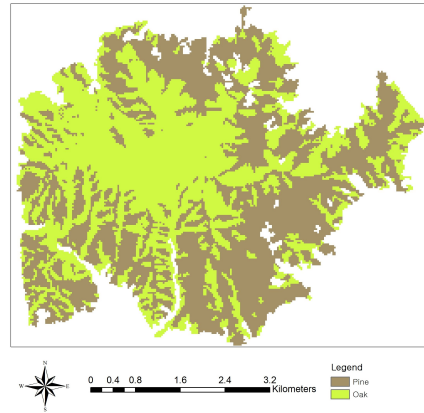


(h)

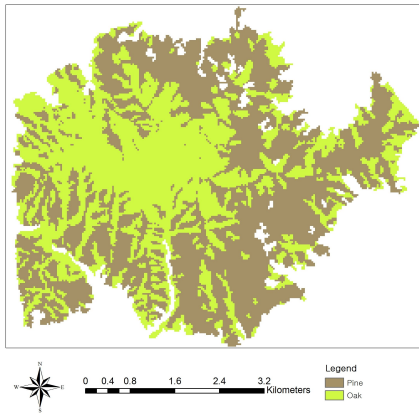
Figure S-1. Pictures of study area. (a) broad-leaved tree, (b) broad-leaved tree, (c) conifer, (d) conifer and broad-leaved tree, (e) conifer and broad-leaved tree, (f) conifer and broad-leaved tree, (g) Landscape of study area, (h) Landscape of study area



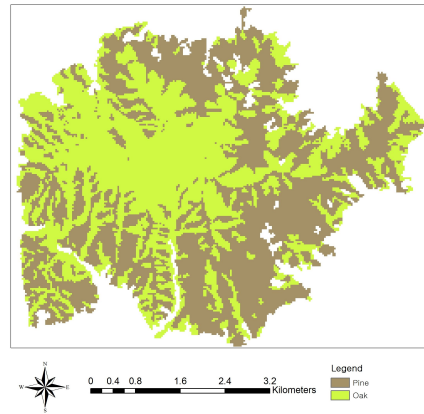
(a)



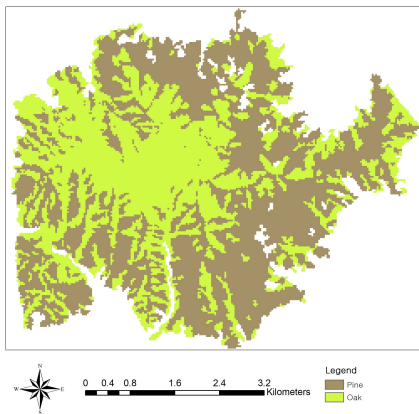
(b)



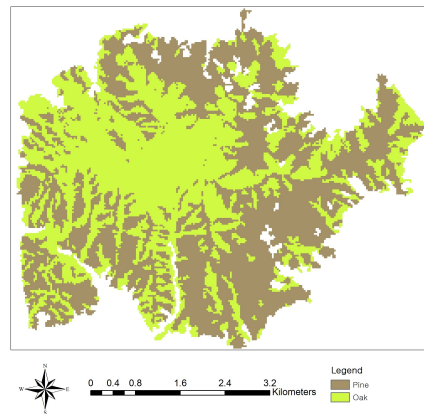
(c)



(d)



(e)



(f)

Figure S-2. Distribution prediction map. (a) 2024 (10%), (b) 2034 (10%), (c) 2024 (average), (d) 2034 (average), (e) 2024 (90%), (f) 2034 (90%)

Summary in Korean

산림 식생 분포는 산림관리의 측면에서 중요하기 때문에 지속적으로 연구되고 있다. 본 연구에서는 과거 상주시 남산의 활엽수림과 침엽수림의 산림분포변화를 분석하고, 이를 바탕으로 미래의 분포 변화를 예측하였다. 과거 분포 변화 분석을 위해 원격탐사를 이용하였으며, 1984년부터 2014년의 분포 변화를 분석하였다. 원격탐사를 위한 위성영상으로는 Landsat 영상을 사용하였으며, 10년 단위로 분포 변화를 분석하였다.

분석결과 상주시 남산은 1984년 이후 침엽수림의 분포가 감소하고 활엽수림의 분포가 증가하고 있으며, 1984년의 경우 과거 활엽수림이 난방용 목재로 이용된 이후 소나무림으로 조림이 이루어져 침엽수림의 분포면적이 넓게 나타났다. 이에 따라 활엽수림은 1984년의 경우 인간 거주 지역 주변에서 거의 분포하지 않는 것으로 나타났으며, 이후 점차 분포면적이 증가하는 양상을 보였다. 이는 과거 소나무림으로 조림된 지역이 활엽수림이 서식하기 적합한 지역이었기 때문에 활엽수림으로의 분포변화양상이 나타난 것으로 판단된다. 또한 대상지의 현재 산림이 대부분 소나무와 참나무류 수종으로 이루어진 것으로 볼 때 시간에 따른 천이양상과 유사한 변화가 나타난 것으로 사료된다.

산림식생의 미래 분포예측을 위한 방법으로 서식 적지를 찾아내는 니체모델, 실제 분포를 예측하기 위한 프로세스 기반과 인구통계학 기반 모델이 있다. 그러나 이런 방법은 산림관리의 측면에서 부족한 점이 있다. 니체 모델의 경우 실제 분포를 예측하기 어렵다는 단점이 있으며, 프로세스 기반과 인구통계학 기반 모델은 상세한 모델 프로세스에 비해 사용할 수 있는 데이터 스케일 및 해상도의 한계가 존재한다. 본 연구에서는 이러한 한계를 극복하여 미래 침엽수림과 활엽수림의 분포를 예측하

고자 하였다.

본 연구에서는 침엽수 분포지역이 활엽수 분포지역으로 변화할 가능성을 이용하여 미래 분포를 예측하였다. 침엽수 분포지역이 활엽수 분포지역으로 변할 가능성은 과거부터 현재까지 분포 변화를 바탕으로 로지스틱 회귀모형을 이용하여 모델링 하였다. 과거 침엽수와 활엽수의 분포지역은 Landsat 영상의 감독분류기법을 통해 구축하였다. 1984-1995, 1995-2005, 2005-2014년의 침엽수림과 활엽수림 분포지역을 비교하여 ‘침엽수림이 활엽수림으로 변한 지역’과 ‘침엽수림 분포가 유지되는 지역’을 도출하였다. 도출된 지역을 종속변수로, 활엽수림 분포지역 경계로부터의 거리, 고도, 경사, TWI(topographic wetness index), 연간 일사량을 독립변수로 하는 로지스틱 회귀분석을 실시하였다.

로지스틱 회귀분석을 위해 도출된 거리 변수는 식생 분포변화에 영향을 미치는 요소로, 종자의 분산 및 종자의 밀도를 반영하는 변수이다. 구축된 변수와 침엽수림이 활엽수림으로 변한 비율간의 관계를 도출한 결과 과거 종자 분산 및 어린 나무의 분포와 성목의 분포 연구결과와 유사한 형태를 나타내어 연구에 적합한 변수로 판단되었다.

그러나 거리 변수는 30m의 격자 스케일에 기반하여 구축되었기 때문에 불확실성이 존재한다. 이런 단점을 극복하기 위하여 로지스틱 회귀모형의 구축 단계에서 몬테카를로 시뮬레이션을 사용하였다. 각 격자간 거리는 시뮬레이션 결과에 기반하여 하위 10%, 평균, 상위 10%로 구분되었고, 각각에 대한 분석을 실시하였다.

로지스틱 회귀분석 결과 연간 일사량과 활엽수림 분포지역 경계로부터의 거리 변수가 가장 영향을 미치는 변수로 도출되었다. 즉, 침엽수림 분포지역이 활엽수림 분포지역으로 변할 가능성은 연간 일사량이 적을수록 높게 나타났으며, 활엽수림 분포지역 경계로부터의 거리가 가까울수록

변화 가능성이 높은 것으로 나타났다. 이는 활엽수림이 침엽수림에 비해 내음성이 강한 특성이 반영되었으며, 종자의 분산 거리에 따른 밀도 변화가 반영된 것으로 판단된다.

구축된 로지스틱 회귀모델을 이용하여 미래 침엽수림과 활엽수림의 분포를 예측하였다. 활엽수림의 분포지역으로 변화하는 침엽수림 분포지역은 점차 줄어들고 있으며, 이는 활엽수림의 분포에 적합한 지역이 줄어들고 있는 것으로 판단된다. 활엽수림의 분포 면적 변화는 개체군 성장 곡선인 시그모이드 형태를 나타내는 것으로 볼 때, 분포변화에 대한 예측이 기존 한정된 자원을 이용하는 개체군 동태의 이론을 반영하는 것으로 사료된다.

결과적으로 종자의 분산을 반영하는 변수를 사용하여 미래 침엽수림과 활엽수림의 분포변화를 예측하였다. 활엽수림 분포지역 경계로부터의 거리 변수를 이용하여 미래 분포변화를 예측하는 것은 적합한 것으로 판단된다. 또한 데이터의 공간해상도로 인하여 발행하는 불확실성은 몬테카를로 시뮬레이션을 활용하여 정량화함으로써 일정부분 극복 가능한 것으로 판단된다.

□ **주요어** : 원격탐사, 로지스틱 회귀분석, 지형보정, 몬테카를로 시뮬레이션, 불확실성

□ **학 번** : 2014-20047